



**HAL**  
open science

## Adaptive diversification through structural variation in barley

Murukarthick Jayakodi, Qiongxian Lu, Helene Pidon, M. Timothy Rabanus-Wallace, Micha Bayer, Thomas Lux, Yu Guo, Benjamin Jaegle, Ana Badea, Wubishet Bekele, et al.

► **To cite this version:**

Murukarthick Jayakodi, Qiongxian Lu, Helene Pidon, M. Timothy Rabanus-Wallace, Micha Bayer, et al.. Adaptive diversification through structural variation in barley. 2024. hal-04493576

**HAL Id: hal-04493576**

**<https://hal.inrae.fr/hal-04493576>**

Preprint submitted on 7 Mar 2024

**HAL** is a multi-disciplinary open access archive for the deposit and dissemination of scientific research documents, whether they are published or not. The documents may come from teaching and research institutions in France or abroad, or from public or private research centers.

L'archive ouverte pluridisciplinaire **HAL**, est destinée au dépôt et à la diffusion de documents scientifiques de niveau recherche, publiés ou non, émanant des établissements d'enseignement et de recherche français ou étrangers, des laboratoires publics ou privés.



Distributed under a Creative Commons Attribution - NonCommercial 4.0 International License

# 1 Adaptive diversification through structural variation in barley

2 Murukarthick Jayakodi<sup>1,31</sup>, Qiongxin Lu<sup>2,31</sup>, H el ene Pidon<sup>1,3,31</sup>, M. Timothy Rabanus-  
3 Wallace<sup>1,31</sup>, Micha Bayer<sup>4</sup>, Thomas Lux<sup>5</sup>, Yu Guo<sup>1</sup>, Benjamin Jaegle<sup>6</sup>, Ana Badea<sup>7</sup>, Wubishet  
4 Bekele<sup>8</sup>, Gurcharn S. Brar<sup>9</sup>, Katarzyna Braune<sup>2</sup>, Boyke Bunk<sup>10</sup>, Kenneth J. Chalmers<sup>11</sup>, Brett  
5 Chapman<sup>12</sup>, Morten Egevang J orgensen<sup>2</sup>, Jia-Wu Feng<sup>1</sup>, Manuel Feser<sup>1</sup>, Anne Fiebig<sup>1</sup>,  
6 Heidrun Gundlach<sup>5</sup>, Wenbin Guo<sup>4</sup>, Georg Haberer<sup>5</sup>, Mats Hansson<sup>13</sup>, Axel Himmelbach<sup>1</sup>,  
7 Iris HOFFIE<sup>1</sup>, Robert E. Hoffie<sup>1</sup>, Haifei Hu<sup>12,14</sup>, Sachiko Isobe<sup>15</sup>, Patrick K onig<sup>1</sup>, Sandip M.  
8 Kale<sup>2</sup>, Nadia Kamal<sup>5</sup>, Gabriel Keeble-Gagn ere<sup>16</sup>, Beat Keller<sup>6</sup>, Manuela Knauft<sup>1</sup>, Ravi  
9 Koppolu<sup>1</sup>, Simon G. Krattinger<sup>17</sup>, Jochen Kumlehn<sup>1</sup>, Peter Langridge<sup>11</sup>, Chengdao Li<sup>12,18</sup>,  
10 Marina P. Marone<sup>1</sup>, Andreas Maurer<sup>19</sup>, Klaus F.X. Mayer<sup>5,20</sup>, Michael Melzer<sup>1</sup>, Gary J.  
11 Muehlbauer<sup>21</sup>, Emiko Murozuka<sup>2</sup>, Sudharsan Padmarasu<sup>1</sup>, Dragan Perovic<sup>22</sup>, Klaus Pillen<sup>19</sup>,  
12 Pierre A. Pin<sup>23</sup>, Curtis J. Pozniak<sup>24</sup>, Luke Ramsay<sup>4</sup>, Pai Rosager Pedas<sup>2</sup>, Twan Rutten<sup>1</sup>, Shun  
13 Sakuma<sup>25</sup>, Kazuhiro Sato<sup>26,15</sup>, Danuta Sch uler<sup>1</sup>, Thomas Schmutzer<sup>19</sup>, Uwe Scholz<sup>1</sup>, Miriam  
14 Schreiber<sup>4</sup>, Kenta Shirasawa<sup>15</sup>, Craig Simpson<sup>4</sup>, Birgitte Skadhauge<sup>2</sup>, Manuel Spannagl<sup>5</sup>,  
15 Brian J. Steffenson<sup>27</sup>, Hanne C. Thomsen<sup>2</sup>, Josquin F. Tibbits<sup>16</sup>, Martin Toft Simmelsgaard  
16 Nielsen<sup>2</sup>, Corinna Trautewig<sup>1</sup>, Dominique Vequaud<sup>23</sup>, Cynthia Voss<sup>2</sup>, Penghao Wang<sup>12</sup>,  
17 Robbie Waugh<sup>4,28</sup>, Sharon Westcott<sup>12</sup>, Magnus Wohlfahrt Rasmussen<sup>2</sup>, Runxuan Zhang<sup>4</sup>,  
18 Xiao-Qi Zhang<sup>12</sup>, Thomas Wicker<sup>6</sup>, Christoph Dockter<sup>2</sup>, Martin Mascher<sup>1,29</sup> & Nils  
19 Stein<sup>1,30</sup>

20 <sup>1</sup>Leibniz Institute of Plant Genetics and Crop Plant Research (IPK) Gatersleben, Seeland,  
21 Germany, <sup>2</sup>Carlsberg Research Laboratory, Copenhagen, Denmark, <sup>3</sup>IPSiM, Univ Montpellier,  
22 CNRS, INRAE, Institut Agro, Montpellier, France, <sup>4</sup>The James Hutton Institute, Dundee,  
23 UK, <sup>5</sup>PGSB - Plant Genome and Systems Biology, Helmholtz Center Munich - German  
24 Research Center for Environmental Health, Neuherberg, Germany, <sup>6</sup>Department of Plant  
25 and Microbial Biology, University of Zurich, Zurich, Switzerland, <sup>7</sup>Brandon Research and  
26 Development Centre, Agriculture et Agri-Food Canada, Brandon, Canada, <sup>8</sup>Ottawa Research  
27 and Development Centre, Agriculture et Agri-Food Canada, Ottawa, Canada, <sup>9</sup>Faculty of  
28 Land and Food Systems, The University of British Columbia, Vancouver, Canada, <sup>10</sup>DSMZ-  
29 German Collection of Microorganisms and Cell Cultures GmbH, Braunschweig,  
30 Germany, <sup>11</sup>School of Agriculture, Food and Wine, University of Adelaide, Urrbrae,  
31 Australia, <sup>12</sup>Western Crop Genetics Alliance, Food Futures Institute/School of Agriculture,  
32 Murdoch University, Murdoch, Australia, <sup>13</sup>Department of Biology, Lund University, Lund,  
33 Sweden, <sup>14</sup>Rice Research Institute, Guangdong Academy of Agricultural Sciences,  
34 Guangzhou, China, <sup>15</sup>Kazusa DNA Research Institute, Kisarazu, Japan, <sup>16</sup>Agriculture Victoria,  
35 Department of Jobs, Precincts and Regions, Agribio, La Trobe University, Victoria, Bundoora,  
36 Australia, <sup>17</sup>Plant Science Program, Biological and Environmental Science and Engineering  
37 Division, King Abdullah University of Science and Technology (KAUST), Thuwal, Saudi  
38 Arabia, <sup>18</sup>Department of Primary Industry and Regional Development, Government of  
39 Western Australia, Perth, Australia, <sup>19</sup>Institute of Agricultural and Nutritional Sciences,  
40 Martin Luther University Halle-Wittenberg, Halle, Germany, <sup>20</sup>School of Life Sciences  
41 Weihenstephan, Technical University Munich, Freising, Germany, <sup>21</sup>Department of  
42 Agronomy and Plant Genetics, University of Minnesota, St. Paul, Minnesota, USA, <sup>22</sup>Institute  
43 for Resistance Research and Stress Tolerance, Julius Kuehn-Institute (JKI), Federal Research  
44 Centre for Cultivated Plants, Quedlinburg, Germany, <sup>23</sup>SECOBRA Recherches, Maule,  
45 France, <sup>24</sup>Department of Plant Sciences and Crop Development Centre, University of

46 Saskatchewan, Saskatoon, SK, Canada, <sup>25</sup>Faculty of Agriculture, Tottori University, Tottori,  
47 Japan, <sup>26</sup>Institute of Plant Science and Resources, Okayama University, Kurashiki,  
48 Japan, <sup>27</sup>Department of Plant Pathology, University of Minnesota, St. Paul, Minnesota,  
49 USA, <sup>28</sup>School of Life Sciences, University of Dundee, Dundee, UK, <sup>29</sup>German Centre for  
50 Integrative Biodiversity Research (iDiv) Halle-Jena-Leipzig, Leipzig, Germany, <sup>30</sup>Center for  
51 Integrated Breeding Research, Georg-August-University, Göttingen, Germany. <sup>31</sup>These  
52 authors contributed equally to this work.

53 ✉ email: [wicker@botinst.uzh.ch](mailto:wicker@botinst.uzh.ch); [christoph.dockter@carlsberg.com](mailto:christoph.dockter@carlsberg.com); [mascher@ipk-](mailto:mascher@ipk-gatersleben.de)  
54 [gatersleben.de](mailto:gatersleben.de); [stein@ipk-gatersleben.de](mailto:stein@ipk-gatersleben.de).

55  
56 **Pangenomes are collections of annotated genome sequences of multiple individuals of a**  
57 **species. The structural variants uncovered by these datasets are a major asset to genetic**  
58 **analysis in crop plants. Here, we report a pangenome of barley comprising long-read**  
59 **sequence assemblies of 76 wild and domesticated genomes and short-read sequence data**  
60 **of 1,315 genotypes. An expanded catalogue of sequence variation in the crop includes**  
61 **structurally complex loci that have become hot spots of gene copy number variation in**  
62 **evolutionarily recent times. To demonstrate the utility of the pangenome, we focus on four**  
63 **loci involved in disease resistance, plant architecture, nutrient release, and trichome**  
64 **development. Novel allelic variation at a powdery mildew resistance locus and population-**  
65 **specific copy number gains in a regulator of vegetative branching were found. Expansion of**  
66 **a family of starch-cleaving enzymes in elite malting barleys was linked to shifts in enzymatic**  
67 **activity in micro-malting trials. Deletion of an enhancer motif is likely to change the**  
68 **developmental trajectory of the hairy appendages on barley grains. Our findings indicate**  
69 **that rapid evolution at structurally complex loci may have helped crop plants adapt to new**  
70 **selective regimes in agricultural ecosystems.**

71  
72 Reliable crop yields fueled the rise of human civilizations. As people embraced a new way of  
73 life, cultivated plants, too, had to adapt to the needs of their domesticators. There are  
74 different adaptive requirements in a wild compared to an arable habitat. Crop plants and their  
75 wild progenitors differ in how many vegetative branches they initiate or how many seeds or  
76 fruits they produce and when. For example, barley (*Hordeum vulgare*) in six-rowed forms of  
77 the crops, thrice as many grains set as in the ancestral two-rowed forms. This change was  
78 brought about by knock-out mutations<sup>1</sup> of a recently evolved regulator<sup>2</sup> of inflorescence  
79 development. Consequently, six-rowed barleys came to predominate in most barley-growing  
80 regions<sup>3</sup>. Taking a broader view of the environment as a set of exogeneous factors that drive  
81 natural selection, barley provides another fascinating, and economically important example.  
82 The process of malting involves the sprouting of moist barley grains, driving the release of  
83 enzymes that break down starch into fermentable sugars. In the wild, various environmental  
84 cues can trigger germination to improve the odds of the emerging seedling encountering  
85 favorable weather conditions for subsequent growth<sup>4</sup>. In the malt house, by contrast,  
86 germination of modern varieties has to be fast and uniform to satisfy the desired specifications  
87 of the industry. In addition to these examples, traits such as disease resistance, plant  
88 architecture and nutrient use have been both a focus for plant breeders and studied  
89 intensively barley geneticists<sup>5</sup>. While barley genetic analyses flourished during a “classical”  
90 period<sup>6</sup> in the first half of the 20th century, it started to lag behind small-genome models due

91 to difficulties in adapting molecular biology techniques to a large genome rich in repeats<sup>7</sup>.  
92 However, interest in barley as diploid model for temperate cereals has surged again as DNA  
93 sequencing became more powerful. High-quality sequences of several barley genomes have  
94 been recently assembled<sup>8</sup>. New sequencing technologies have shifted the focus of barley  
95 genomics: from the modest ambition of a physical map of all genes to a “pangenome”, i.e.  
96 near-complete sequence assemblies<sup>9</sup> of many genomes. Here, we report a pangenome  
97 comprising 76 chromosome-scale sequences assembled from long-reads as well as short-read  
98 sequences of 1,315 barley genomes. These data in conjunction with genetic and genomic  
99 analyses provide insights into the effects of structural variation at loci related to crop evolution  
100 and adaptation.

101

### 102 *An expanded annotated pangenome of barley*

103

104 As in previous diversity studies<sup>8,10</sup>, we aimed for a judicious mix of representativeness,  
105 diversity and integration with community resources (**Fig. 1a**, **Extended Data Fig. 1a-c**,  
106 **Supplementary Table 1**). We selected (i) diverse domesticated germplasm with a focus on  
107 genebank accessions from barley’s center of diversity in the Middle East; (ii) 23 accessions of  
108 barley’s conspecific wild progenitor *H. vulgare* subsp. *spontaneum* from across that taxon’s  
109 geographic range (**Extended Data Fig. 1d**); and (iii) cultivars of agronomic or scientific  
110 relevance. Examples of the last category are Bonus, Foma and Bowman, three parents of  
111 classical mutants<sup>11</sup>. Genome sequences of each accession were assembled to contig-level  
112 from PacBio HiFi accurate long reads<sup>12</sup> and scaffolded with conformation capture sequencing  
113 (Hi-C) data<sup>13</sup> to chromosome-scale pseudomolecules (**Extended Data Fig. 2a**, **Supplementary**  
114 **Table 1**). Gene models were annotated with the help of transcriptional evidence and  
115 homology. Illumina RNA sequencing and PacBio isoform sequencing of five different tissues  
116 (**Supplementary Table 2**) were generated for 20 accessions. Gene models predicted in these  
117 genomes were projected onto the remaining 56 sequence assemblies (**Supplementary Table**  
118 **3**). Out of 4,896 single-copy genes conserved across the Poales, on average fewer than 92  
119 (1.9%) were absent in the pangenome annotations (**Supplementary Table 3**). Our assemblies  
120 also met the other quality metrics proposed by the EarthBiogenome project<sup>14</sup>  
121 (**Supplementary Table 1**).

122

### 123 *An atlas of structural variation*

124

125 Gene content variation was abundant in the barley pangenome. The gene models in the 76  
126 genomes were clustered into 95,735 orthologous groups (**Extended Data Fig. 3**), of which only  
127 16,672 (17.4%) were present in all 76 genotypes. Of these groups, 14,736 had a single  
128 representative in each of the genomes. At the level of individual gene models, a third were  
129 considered conserved because they belong to an orthologous group with representatives  
130 from each accession (**Extended Data Fig. 3b**). As expected for conspecific populations  
131 connected by gene flow, wild and domesticated barleys were not strongly differentiated in  
132 their gene content: of 78,565 orthologous groups subject to presence/absence variation, only  
133 863 and 397 were private to wild and domesticated barleys, respectively. The functional  
134 annotations of clusters restricted to specific gene pools (wild forms, landraces, cultivars and  
135 combinations of these groups) pointed to an involvement in biotic and abiotic stress responses  
136 (**Supplementary Table 4**).



137 To expand the catalogue of presence/absence variants (PAV), insertion and deletions (indels)  
138 and polymorphic inversions, we aligned the genome sequences and detected structural  
139 variants (**Fig. 1b**, **Extended Data Fig. 2b-d**, **Extended Data Fig. 3c**). Noteworthy were two  
140 reciprocal interchromosomal translocations, the first in HOR 14273, an Iranian landrace, and  
141 the second in HID055, a wild barley from Turkey (**Fig. 1b**). The latter event joins the short arm  
142 of chromosome 2H with the long arm of chromosome 4H (and vice versa) and manifests itself  
143 in a biparental population between HID055 and Barke<sup>15</sup> in interchromosomal linkage (**Fig. 1c**)  
144 and incomplete seed set in the offspring. This illustrates that inadvertent selection of  
145 germplasm with structural variants can create obstacles for the use of plant genetic resources.  
146 The presence of both wild and domesticated barleys in our panel made it possible to compare  
147 the levels of structural diversity in the two taxa. Graph structures tabulating the presence and  
148 absence of single-copy loci in individual genomes<sup>8</sup> grew faster in wild than in cultivated forms  
149 (**Fig. 1d**): a larger amount of single-copy sequence was present in 23 wild barley genomes than  
150 in 53 genomes of the domesticate. This pattern was also seen in a whole-genome graph  
151 constructed with minigraph<sup>16</sup> (**Extended Data Fig. 4e**). The pangenome graph improves the  
152 accuracy of read alignment and variant calling: more reads were aligned as proper pairs, and  
153 with fewer mismatches, to the graph than to a single reference genome (**Extended Data Fig.**  
154 **4b**). The genome-wide distribution of structural variants encapsulated in the graph matched  
155 that inferred from pairwise alignments (**Extended Data Fig. 4c-d**). However, owing to high  
156 computational requirements<sup>17</sup>, pangenome graph construction with packages supporting  
157 small variants (< 50 bp) is still computationally prohibitive in barley.  
158 Despite domestication bottlenecks, genetic diversity is high in cultivated barley<sup>5</sup>. To quantify  
159 the completeness of the haplotype inventory of our pangenome, we compared our  
160 assemblies against short-read data of a global diversity panel (**Supplementary Table 5**). A core  
161 set of 1,000 genotypes selected from a collection of 22,626 barleys<sup>3</sup> was sequenced to three-  
162 fold haploid genome coverage. Nested therein, 200 genomes<sup>8</sup> were sequenced to 10-fold  
163 depth and the gene space of 46 accessions was represented in the contigs assembled from  
164 50-fold short-read data (**Extended Data Fig. 5a**, **Supplementary Table 6**). A total of 315 elite  
165 cultivars of European ancestry were sequenced to 3-fold coverage (**Extended Data Fig. 5a**,  
166 **Supplementary Table 5**). More than 164.5 million single-nucleotide polymorphisms (SNPs)  
167 and indels were detected across all panels (**Extended Data Fig. 5b**). Overlaying these with the  
168 pangenome showed that the 76 chromosome-scale assemblies captured almost all pericentric  
169 haplotypes of cultivated barley (**Extended Data Fig. 2d-f**). Coverage decreased to as low as  
170 50% in distal regions, where haplotypes of plant genetic resources lacked a close relative in  
171 the pangenome more often than those of elite cultivars (**Extended Data Fig. 2e-f**). This  
172 suggests that, thanks to broad taxon sampling, short-read sequencing will remain  
173 indispensable for the time being, but in the future population-scale long-read sequencing<sup>18</sup>  
174 will be a desirable in agricultural genetics as it is in medical genetics.

#### 175 176 *An inventory of complex loci*

177  
178 Long-read sequencing has the power to resolve structurally complex genomic regions, where  
179 repeated cycles of tandem duplication, mutation of duplicated genes and elimination by  
180 deletion or recombination have created a panoply of diverged copies of one or multiple genes  
181 in varied arrangements (**Extended Data Fig. 6a**). Many complex loci are intimately linked to  
182 the evolution of resistance genes<sup>19</sup>. An illustrative example is barley's *Mildew resistance locus*  
183 *a* (*Mla*)<sup>20,21</sup>, which contains three families of resistance gene homologs, each with multiple

184 members at the locus. A 40 kb region containing members of two families is repeated four  
185 times head-to-tail in RGT Planet, but is not present in even a single complete copy in 62  
186 accessions of our pangenome (**Extended Data Fig. 6b-c**). *Mla* genes *sensu strictu*, i.e. those  
187 that have been experimentally proven to provide functional powdery mildew resistance, are  
188 among members of a subfamily that resides outside of this duplication but close to its distal  
189 border (**Fig. 2a-b, Extended Data Fig. 6b-c**). Twenty-nine *Mla* alleles in the narrow sense have  
190 been defined to date<sup>22</sup>. Gene models identical to seven were identified in our pangenome  
191 (**Fig. 2a**). However, the sequence variation went beyond this observation: 149 unique gene  
192 models were different from, but highly similar to known *Mla* alleles, with nucleotide  
193 sequences at least 98% identical. Some of these genes were present in multiple copies. HOR  
194 8117, a landrace from Nepal, contained 11 different close homologs of *Mla*, two of which were  
195 present in five copies each (**Supplementary Fig. 1**). Genome sequences alone cannot inform  
196 us how this sequence diversity relates to resistance to powdery mildew or other diseases<sup>23</sup>.  
197 Until the advent of long-read sequencing, it was virtually impossible to resolve the structure  
198 of the *Mla* locus in multiple genomes at once, but now it is a corollary of pangenomics.  
199 We employed a gene-agnostic method<sup>24</sup> to scan the genome sequence of Morex for  
200 structurally complex loci harbouring genes, focusing on examples that had evidently caused  
201 gene copy number variation across the pangenome via the expansion or collapse of long  
202 tandem repeats. A total of 173 loci ranging in size from 20 kb to 2.2 Mb (median: 125 kb)  
203 matched our criteria (**Fig. 2c, Supplementary Table 7**). Their copy numbers were variable in  
204 the pangenome. The most extreme case was a cluster of genes annotated by homology as  
205 thionin genes, which are possibly involved in resistance to herbivory<sup>25</sup>. The locus had as few  
206 as three thionin gene copies in the wild barley WBDC103 and up to 78 copies in WBDC199,  
207 another wild barley (**Extended Data Fig. 6d**). Genes associated with such complex loci  
208 possessed functional annotations suggesting involvement in various biological processes (**Fig.**  
209 **2c, Supplementary Table 7**). Complex loci were enriched in distal chromosomal regions (**Fig.**  
210 **2d**). In this regard, they follow the same distal-to-proximal gradient as genetic diversity and  
211 recombination frequency. The latter process might play a role in their amplification and  
212 contraction owing to unequal homologous recombination between neighboring repeat units<sup>26</sup>  
213 (**Extended Data Fig. 6a**). Molecular dating of the tandem duplications in Morex is consistent  
214 with rapid evolution (**Extended Data Fig. 7**): loci with many gene copies appear to have gained  
215 them within the last three million years (**Extended Data Fig. 7c**), after the *H. vulgare* lineage  
216 split from that of its closest relative *H. bulbosum*<sup>27</sup>. In addition, 63 loci (36.4%) underwent at  
217 least one duplication in the last 10,000 years, that is, after domestication (**Extended Data Fig.**  
218 **7d**). Forty-five loci expanded so recently that the genes they harboured were identical  
219 duplicates of each other.  
220 One interesting case of such recent diversification was a duplication at the *HvTB1* locus (also  
221 known as *INTERMEDIUM-C* [*INT-C*] or *SIX ROWED SPIKE 5*). *HvTB1* is a TEOSINTE BRANCHED  
222 1, CYCLOIDEA, PCF1 (TCP) transcription factor involved in basal branching (tillering) and other  
223 aspects of plant architecture in cereal grasses<sup>28-30</sup>. In barley, both tillering and the fertility of  
224 lateral spikelets is increased in knock-out mutants<sup>30,31</sup>. Just two alleles, *Int-c.a* and *int-c.b*.  
225 dominate in six-rowed and two-rowed forms<sup>30</sup>, respectively, and *HvTB1* is not genetically  
226 linked to the *SIX ROWED SPIKE 1* gene. Both alleles of *HvTB1* are thought to be functional and  
227 occur also in wild barley<sup>30,32</sup>. These patterns have defied easy explanation. Expression  
228 differences owing to regulatory variation have been postulated but not proven<sup>30</sup>. The  
229 pangenome adds another twist. *HvTB1* is a single-copy gene in all 22 *H. spontaneum*  
230 accessions and 23 two-rowed domesticates except HOR 7385 (**Supplementary Table 8**). Six-

231 rowed forms, however, have up to four copies of a 21 kb segment that contains *HvTB1* and ~5  
232 kb of its upstream sequence (**Fig. 2b**). The reference cultivar Morex has three copies, although  
233 these were falsely collapsed in previous short-read assemblies of that variety<sup>33</sup>. On top of  
234 variable copy numbers, the pangenome revealed six hitherto unknown HvTB1 protein variants  
235 (**Extended Data Fig. 6d, Supplementary Table 8**). Reduced tillering in maize has been  
236 attributed to overexpression of *TB1*. The barley pangenome will help developmental  
237 geneticists reveal if copy number gains had analogous effects in six-rowed forms.

238

### 239 *Amplification of $\alpha$ -amylases in malting barley*

240

241 Among the complex loci we examined, the *amy1\_1* locus of  $\alpha$ -amylases is arguably the one of  
242 greatest economic importance. These enzymes cleave the polysaccharide starch into short-  
243 chain forms, which are then digested further into sugars<sup>34</sup>. In both wild and cultivated forms,  
244 the speed and efficiency of that process determines the energy supply to and hence the vigor  
245 of the young seedling<sup>35</sup>. In grains of domesticated barley, the enzymatic conversion of starch  
246 into fermentable sugars by  $\alpha$ -amylases initiates the malting process. Barley  $\alpha$ -amylases are  
247 subdivided into four families, which occupy distinct genomic loci (**Extended Data Fig. 8a,**  
248 **Supplementary Tables 9 and 10**). Earlier genome sequences assembled from short reads  
249 hinted at the presence of structural variation at the *amy1\_1* locus on chromosome 6H,  
250 respectively, but failed to resolve copy numbers<sup>36</sup>. By contrast, each of our long-read  
251 assemblies covered *amy1\_1* in a single contig (**Extended Data Fig. 9a**). Copy numbers of  
252 *amy1\_1* in 76 complete genomes varied between two and eight, with on average more copies  
253 in domesticated than in wild forms (**Fig. 3a, b**). Individual copies were addressable by 21-mers  
254 that overlap sequence variants. We counted these 21-mers in the short-reads of 1,315  
255 genotypes and also determined SNP haplotypes around the *amy1\_1* locus in these data  
256 (**Extended Data Figs. 8e-f, 9b, Supplementary Tables 11 and 12**). Eight clusters were  
257 discernible and could be related to population structure. Three-quarters of hulless barleys  
258 were in cluster #7. Six-rowed barleys belonged mostly to clusters #1 and #6. Among 315  
259 European varieties, clusters #5 and #6 were most common. Clusters #3 and #8 with fewer  
260 *amy1\_1* copies were exclusive to plant genetic resources. Barleys from eastern and central  
261 Asian countries tend to have high copy numbers. *Amy1\_1* copy numbers were higher on  
262 average in elite varieties than in other barleys (**Fig. 3b**). Structural diversity was accompanied  
263 by differences in gene sequence owing to SNPs and indels in open reading frames and  
264 promoters. The 76 genome assemblies had 94 distinct *amy1\_1* haplotypes (**Fig. 3c, Extended**  
265 **Data Fig. 8b, Supplementary Tables 13-16**). Twelve had insertions of transposable elements  
266 (**Supplementary Table 17**). At the protein level, there were 38 unique AMY1\_1 isoforms  
267 (**Supplementary Tables 18 and 19**), some of which were predicted to affect protein<sup>37</sup> stability  
268 and thereby influence  $\alpha$ -amylase activity (**Fig. 3d, e**).

269 We investigated in more detail the elite malting barleys Morex, Barke and RGT Planet (**Fig. 3,**  
270 **Supplementary Tables 20 and 21**). Prior to its use as a genome reference cultivar, Morex was  
271 a successful variety in North America. It had six nearly identical (> 99 % similarity) *amy1\_1*  
272 copies. (**Fig. 3a**). The fifth copy was disrupted by the insertion of a transposable element. Full-  
273 length copies were verified by PacBio amplicon sequencing. Barke, a European cultivar, had  
274 six full-length copies, albeit of a different haplotype. RGT Planet, currently a successful cultivar  
275 in many barley-growing regions around the world, had five copies, one of which was likely to  
276 be inactivated by a 32 bp deletion in a pyr-box (CTTT(A/T) core) promoter binding site that is  
277 essential for  $\alpha$ -amylase transcription<sup>38</sup>. We tested overall  $\alpha$ -amylase activity in micro-malting

278 trials with RGT Planet and near-isogenic lines (NILs) that carried Morex and Barke *amy1\_1*  
279 haplotypes in the genomic background of RGT Planet. It was observed that  $\alpha$ -amylase activity  
280 was highest in *amy1\_1*-Barke NILs (**Fig. 3e**). The Barke haplotype is common not only in  
281 cultivars favored by European maltsters, but also among those from other regions of the  
282 world, where barley  $\alpha$ -amylases need to be abundant enough to cleave starch from adjuncts  
283 such as maize and rice (**Supplementary Table 22**). The patterns of sequence variation at  
284 *amy1\_1* uncovered by the barley pangenome pave the way for the targeted deployment,  
285 possibly even design, of *amy1\_1* haplotypes in breeding.

286

### 287 *A regulatory variation controls trichome development*

288

289 Our last example sits at the intersection of developmental genetics, breeding and  
290 domestication. Hairy appendages to grains and awns are conducive to seed dispersal in wild  
291 plants, but have lost this function in domesticates<sup>39</sup>. A pertinent example are the hairs on the  
292 rachillae of barley grains. In barley, the rachilla is the rudimentary secondary axis of the  
293 inflorescence, where multiple grains are set in wheat<sup>40</sup>. In the single-grained spikelets of  
294 barley, the rachilla is a thin and hairy thread-like structure nested in the ventral crease of the  
295 grains. The long hairs of the rachillae of wild barleys and most cultivated forms are unicellular,  
296 while the short hairs of some domesticated types are multicellular and branched (**Fig. 4a**,  
297 **Extended Data Fig. 10a**). This seemingly minor difference in a vestigial organ belies its  
298 importance in variety registration trials<sup>41</sup>, where breeders would like to predict the trait with  
299 a diagnostic marker. *Short rachilla hair 1* (*srh1*) is also a classical locus in barley genetics<sup>42</sup>. It  
300 has been mapped genetically<sup>8,43</sup> (**Fig. 4b**) and both long- and short-haired genotypes are  
301 included in our pangenome. Fine-mapping in a population of 2,398 recombinant inbred lines  
302 derived from a cross<sup>36,44</sup> between cultivars Morex (short, *srh1*) and Barke (long, *Srh1*)  
303 delimited the causal variant to a 113 kb interval on the long arm of chromosome 5H (**Fig. 4c**,  
304 **Supplementary Table 23**). Outside of this interval (which is itself devoid of annotated gene  
305 models), but within 11 kb of the distal flanking marker is a homolog of a *SIAMESE-RELATED*  
306 (*SMR*) gene of the model plant *Arabidopsis thaliana*<sup>45,46</sup>. Members of this family of cyclin-  
307 dependent kinase inhibitors control endoreduplication in trichomes of that species. In barley,  
308 hair cell development is likewise accompanied by endopolyploidy-dependent cell size  
309 increases (**Extended Data Fig. 10b**). The *SMR*-homolog was expressed in the rachilla's  
310 developing trichomes (**Extended Data Fig. 10e**), but there were no differences between Morex  
311 and Barke in the sequence of this otherwise plausible candidate gene. Despite this conflicting  
312 evidence, we proceeded with mutational analysis and obtained several mutants using FIND-  
313 IT<sup>47</sup> (**Extended Data Fig. 10c,d**) and Cas9-mediated targeted mutagenesis (**Fig. 4d**,  
314 **Supplementary Fig. 2, Supplementary Tables 24 and 25**). Mutants of long-haired genotypes  
315 with knock-out variants or a nonsynonymous change in a Pro phosphorylation motif (Thr62-  
316 Pro63) had short, multicellular rachillae, supporting the idea that the gene in question,  
317 *HORVU.MOREX.r3.5HG0492730*, is indeed *HvSRH1*. Sequence variants in *HvSRH1* identified in  
318 the pangenome did not lend itself to easy explanation: 18 protein haplotypes caused by 23  
319 non-synonymous variants bore no obvious relation to the phenotype (**Supplementary Table**  
320 **26**). Thus, we then examined regulatory variation. All 14 short-haired genotypes in the  
321 pangenome lacked a 4,273 bp sequence (**Fig. 4c**), which was exceptionally well conserved in  
322 long-haired types, with 95% overall identity to Barke. Within this sequence, we found the  
323 motif CATCGGATCCTT, matching the sequence [ATC]T[ATC]GGATNC[CT][ATC], which is  
324 recognized by regulators of *SMR* expression in *A. thaliana*<sup>48</sup>. That sequence was repeated five



325 times in Barke. The closest unit in long-haired types was no further than 13.6 kb from the  
326 gene, while the minimum distance between the gene and its putative enhancer motif in short-  
327 haired types was 22.3 kb, owing to the 4.3 kb deletion (**Fig. 4c**). *HvSRH1* expression during  
328 rachilla hair elongation is higher in long-haired than in short-haired genotypes (**Extended Data**  
329 **Fig. 10f**). Gene edits of the enhancer region, guided by the pangenome sequences, will further  
330 elucidate the transcriptional regulation of *HvSRH1*.

331

### 332 *Discussion*

333

334 The recently published human draft pangenome demonstrated how contiguous long-read  
335 sequences help make sense of reams of sequence data<sup>49</sup>. Our study on barley pangenome  
336 sheds light on crop evolution and breeding. The shortcomings of previous short-read  
337 assemblies made it all but impossible to see patterns that now emerge from their long-read  
338 counterparts. We were able for the first time to study the evolution of structurally complex  
339 loci of nearly identical tandem repeats. Our developmental insights are admittedly still  
340 cursory: true to the hypothesis-generating remit of genomics, and at least as many questions  
341 were raised as answered. We studied four loci – *Mla*, *HvTB1*, *amy1\_1*, *HvSRH1* – and the traits  
342 they control: disease resistance, plant architecture, starch mobilization and the hairiness of a  
343 rudimentary appendage to the grain. In two of these examples, phenotypic diversity has  
344 visibly increased in domesticated forms: there are no six-rowed or short-haired wild barleys.  
345 Malting created new selective pressures that only cultivated forms experienced. Novel allelic  
346 variation at disease resistance loci is both illustrative of the power of pangenomics and in line  
347 with our understanding of how disease resistance genes evolve. Structural variation at  
348 *amy1\_1* has been known for some time, but previous attempts at resolving the structure of  
349 the locus had been thwarted by incomplete genome sequences. Tandem duplications and  
350 deletions of regulatory elements, respectively, at *HvTB1* and *HvSRH1* was surprising since for  
351 many years barley geneticists considered the loci as monofactorial recessive. Much of the  
352 variation seems to have arisen after domestication, either because mutations that appear with  
353 clock-like regularity were absent or copy numbers were lower in the wild progenitor than in  
354 the domesticated forms. A common concern among crop conservationists is dangerously  
355 reduced genetic diversity in cultivated plants<sup>50</sup>. But crop evolution need not be a  
356 unidirectional loss of diversity. This study has shown that valuable diversity can arise after  
357 domestication. Rapid evolution at structurally complex loci may endow domesticated plants  
358 with a means of adaptive diversification that aptly fulfills the needs of farmers and breeders.  
359 More diverse crop pangenomes will help us understand how the counteracting forces of past  
360 domestication bottlenecks and newly arisen structural variants influence future crop  
361 improvement in changing climates.

362

### 363 **Acknowledgments**

364 We are grateful for the technical assistance of Susanne König, Ines Walde, Sabine Sommerfeld,  
365 John Fuller, Nicola McCallum and Malcolm Macaulay and thank Thomas Münch, Jens  
366 Bauernfeind and Heiko Mieke for IT administration. Andreas Börner supported the  
367 development of the core1000 diversity panel. Sequencing of Chikurin Ibaraki 1 was performed  
368 at the Institute for Clinical Molecular Biology, Competence Centre for Genomic Analysis  
369 (CCGA), Kiel University, Kiel, Germany under the supervision of Dr. Janina Fuß. Sequencing of  
370 HOR 4224 was performed at Genomics & Transcriptomics Labor (BMFZ) Heinrich-Heine-  
371 Universität, Universitätsklinikum Düsseldorf, Germany under the supervision of Prof. Dr. Karl

372 Köhrer. RGT Planet and Maximus were sequenced at Genomics WA under the supervision of  
373 Dr. Alka Saxena and at Novogene, respectively. N.S., M.M., K.F.X.M., M.Spannagl and U.S. were  
374 supported by grants from the German Ministry of Research and Education (BMBF, 031B0190  
375 and 031B0884). D.P. was supported by BMBF grant 031B0199B and the German Federal  
376 Ministry of Food and Agriculture (grant 2818BIJP01). U.S.'s research is supported by the  
377 German Research Foundation (DFG, grant 442032008). C.D., Q.L., P.R.P. and B.S. gratefully  
378 acknowledge support from the Carlsberg Foundation to B.S. (grants CF15-0236, CF15-0476,  
379 CF15-0672) and thank F. Lok, S. Knudsen, G. B. Fincher and K. G. Jørgensen for providing  
380 valuable scientific thoughts and discussions on barley  $\alpha$ -amylases and malt quality. R.W., M.B.,  
381 M.Schreiber, W.G., R.Z. and C.S. received funding from the Rural and Environment Science and  
382 Analytical Services Division (RESAS, grant KJHI-B1-2). W.G. and R.Z. were supported by grant  
383 BB/S020160/1 from the Biotechnology and Biological Sciences Research Council (BBSRC). C.P.  
384 acknowledges support from Genome Canada and Genome Prairie. B.K. acknowledges a grant  
385 from the Swiss National Science Foundation (310030\_204165). C.L., K.C. and P.L. were  
386 supported by a grant from the Grain Research and Development Corporation (UMU1806-  
387 002RTX), by the Department of Primary Industry and Regional Development Western Australia  
388 and by Pawsey Australia (for computational resources). K.P. and T.S. received a grant from DFG  
389 (HAPPAN, 433162815). G.S.B. has received support from the Saskatchewan Ministry of  
390 Agriculture (grant ADF20200165) and from the Saskatchewan Barley Development  
391 Commission, Western Grains Research Foundation, Alberta Barley Commission and the  
392 Manitoba Crop Alliance (grant ADF20210677). A.B. and W.B. are recipients of the TUGBOAT  
393 grant from the Agriculture and Agri-Food Canada – Genomics Research and Development  
394 Initiative and the grant “Unlocking barley endophyte microbiome to enhance plant health and  
395 grain quality” from Agriculture and Agri-Food Canada – A-Base – Foundational Science. M.H.  
396 is supported by the Swedish Research Council (VR 2022-03858), the Swedish Research Council  
397 for Environment, Agricultural Sciences, and Spatial Planning (FORMAS 2018-01026), the Erik  
398 Philip-Sörensen Foundation and the Royal Physiographic Society in Lund. K.Sato's research is  
399 funded by the Japan Science and Technology Agency (grant no. 18076896) and the Japan  
400 Society for the Promotion of Science (JSPS, grant no. 23H00333). K.Shirasawa is supported by  
401 the JSPS grants nos. 22H05172 and 22H05181. S.S. acknowledges the Research Support  
402 Project for the Next Generation at Tottori University. B.S. is supported by the Lieberman-  
403 Okinow Endowment at the University of Minnesota and S.G.K. by baseline funding at KAUST.  
404 The authors acknowledge the Research/Scientific Computing teams at The James Hutton  
405 Institute and NIAB for providing computational resources and technical support for the "UK's  
406 Crop Diversity Bioinformatics HPC" (BBSRC grant BB/S019669/1), use of which has contributed  
407 to the results reported in this paper.

408

#### 409 **Author contributions**

410 N.S. and M.Mascher designed the study. N.S. coordinated experiments and sequencing.  
411 M.Mascher and M.J. supervised sequence assembly. M.Spannagl and K.F.X.M. supervised  
412 annotation. U.S. supervised data management and submission. Selection of genotypes: A.B.,  
413 W.B., G.S.B., K.J.C., Y.G., M.H., B.K., S.G.K., P.L., C.L., M.Mascher, A.M., G.J.M., D.P., K.P., C.J.P.,  
414 S.S., K.Sato, T.S., B.S., N.S., R.W. Genome sequencing: B.B., A.H., S.I., M.K., C.L., S.P., S.S., K.Sato,  
415 T.S., M.Schreiber, K.Shirasawa, N.S., S.W., X.Z. Sequence assembly: B.C., H.H., M.J., G.K.-G.,  
416 M.Mascher, S.P., K.Sato, T.S., J.F.T. Transcriptome sequencing and analysis: W.G., A.H., S.P., C.S.,  
417 N.S., R.Z. Annotation: H.G., G.H., N.K., T.L., K.F.X.M., M.Spannagl. Analysis and interpretation  
418 of structural variants: M.B., B.C., J.-W.F., Y.G., M.J., C.L., M.P.M., A.M., S.P., H.P., K.P., T.S.,



419 M.Schreiber, P.W. Analysis of complex loci: B.J., B.K., M.T.R.-W., N.S., T.W. Analysis of *amy1\_1*  
420 locus: K.B., C.D., M.E.J., B.J., M.J., S.M.K., Q.L., M.P.M., E.M., P.A.P., P.R.P., B.S., H.C.T., M.T.S.N.,  
421 D.V., C.V., M.W.R. *srh1* analysis: C.D., M.E.J., I.H., R.E.H., M.J., R.K., J.K., Q.L., M.Melzer, H.P.,  
422 L.R., P.R.P., T.R., B.S., N.S., H.C.T., C.T., C.V., M.W.R. Data management and submission: M.B.,  
423 M.F., A.F., M.J., P.K., M.Mascher, D.S., U.S. Writing: M.B., C.D., M.E.J., M.J., Q.L., M.Mascher,  
424 N.S., T.W. Coordination: C.D., M.Mascher, N.S. All authors read and commented on the  
425 manuscript.

426

#### 427 **Competing interests**

428 K.B., C.D., M.E.J., S.M.K., Q.L., E.M., P.R.P., B.S., H.C.T., M.T.S.N., C.V., M.W.R. are current or  
429 previous Carlsberg A/S employees. P.A.P. and D.V. are SECOBRA Recherches employees. All  
430 other authors declare no competing interests.

431

#### 432 **List of supplementary items**

433

434 **Supplementary Figure 1:** Structure and copy number variation at *Mla* at different thresholds  
435 for alignment similarity.

436 **Supplementary Figure 2:** Targeted mutagenesis at *HvSRH1*.

437 **Supplementary Table 1:** Passport data of 76 genotypes and statistics and accession codes of  
438 their long-read assemblies

439 **Supplementary Table 2:** Accession codes of transcriptome data

440 **Supplementary Table 3:** Gene annotation statistics

441 **Supplementary Table 4:** Gene ontology enrichment in genepool-specific orthologous groups

442 **Supplementary Table 5:** Passport data of 1,315 genotypes sequenced with short reads,  
443 accession codes and mapping stats

444 **Supplementary Table 6:** Statistics and accession codes of 46 gene-space assemblies

445 **Supplementary Table 7:** List of 173 structurally complex loci.

446 **Supplementary Table 8:** Allelic profiles of 76 barley accessions at the 4H\_015772 locus (*Int-*  
447 *c*) and at *Vrs1*.

448 **Supplementary Table 9:**  $\alpha$ -amylase gene IDs and chromosomal locations in Morex.

449 **Supplementary Table 10:** Sequence identity matrix of germination-related *amy1*, *amy2* and  
450 *amy3* genes in the Morex genome. *amy4* genes involved in general starch metabolism were  
451 excluded due to low sequence identity with other  $\alpha$ -amylases.

452 **Supplementary Table 11:** SNP haplotype clustering analyses and k-mer based *amy1\_1* copy  
453 number estimation in 1,000 plant genetic resources

454 **Supplementary Table 12:** SNP haplotype clustering analyses and k-mer based *amy1\_1* copy  
455 number estimation in 315 European elite cultivars

456 **Supplementary Table 13:** Overview of *amy1\_1* unique ORFs (start to stop codon including  
457 intron). HORVU.MOREX.PROJ.6HG00545380 was used as the reference.

458 **Supplementary Table 14:** Overview of *amy1\_1* ORF haplotypes (ORFHap#).

459 **Supplementary Table 15:** Overview of *amy1\_1* unique CDS.

460 HORVU.MOREX.PROJ.6HG00545380 was used as the reference.

461 **Supplementary Table 16:** Overview of *amy1\_1* CDS haplotypes (CDSHap#).

462 **Supplementary Table 17:** *amy1\_1* genes with insertions of transposable elements in the  
463 genome assemblies.

464 **Supplementary Table 18:** Overview of *amy1\_1* unique proteins.

465 HORVU.MOREX.PROJ.6HG00545380 was used as the reference.

- 466 **Supplementary Table 19:** Overview of *amy1\_1* protein haplotypes (ProtHap#).  
467 **Supplementary Table 20:** Amino acid variation in three *amy1\_1* haplotypes commonly found  
468 in elite varieties (Morex, Barke and RGT Planet).  
469 **Supplementary Table 21:** DynaMut2 prediction of protein stability changes by amino acid  
470 variants found in three BPGv2 representatives of widely used *amy1\_1* haplotypes found in  
471 elite breeding material (Morex, Barke and RGT Planet).  
472 **Supplementary Table 22:** *amy1\_1*-Barke haplotype genotyping of AMBA(American Malting  
473 Barley Association)-recommended two-row spring malting barley varieties accredited for  
474 adjunct brewing.  
475 **Supplementary Table 23:** PACE markers designed in this study.  
476 **Supplementary Table 24:** Oligonucleotides used for gRNA cloning and for PCR amplification  
477 of the target region.  
478 **Supplementary Table 25:** Summary of lesions induced in *HvSRH1* by Cas9-mediated targeted  
479 mutagenesis.  
480 **Supplementary Table 26:** *srh1* phenotypes and *HvSRH1* gene coordinates in 76 pangenome  
481 accessions.

482

## 483 References

484

- 485 1 Komatsuda, T. *et al.* Six-rowed barley originated from a mutation in a homeodomain-  
486 leucine zipper I-class homeobox gene. *Proceedings of the National Academy of*  
487 *Sciences* **104**, 1424-1429 (2007). <https://doi.org/10.1073/pnas.0608580104>  
488 2 Sakuma, S. *et al.* Divergence of expression pattern contributed to  
489 neofunctionalization of duplicated HD-Zip I transcription factor in barley. *New*  
490 *Phytologist* **197**, 939-948 (2013). <https://doi.org/10.1111/nph.12068>  
491 3 Milner, S. G. *et al.* Genebank genomics highlights the diversity of a global barley  
492 collection. *Nat Genet* **51**, 319-326 (2019). [https://doi.org/10.1038/s41588-018-0266-](https://doi.org/10.1038/s41588-018-0266-x)  
493 [x](https://doi.org/10.1038/s41588-018-0266-x)  
494 4 Abbo, S. *et al.* Plant domestication versus crop evolution: a conceptual framework for  
495 cereals and grain legumes. *Trends in Plant Science* **19**, 351-360 (2014).  
496 <https://doi.org/10.1016/j.tplants.2013.12.002>  
497 5 Dawson, I. K. *et al.* Barley: a translational model for adaptation to climate change.  
498 *New Phytol* **206**, 913-931 (2015). <https://doi.org/10.1111/nph.13266>  
499 6 Lundqvist, U. Scandinavian mutation research in barley – a historical review.  
500 *Hereditas* **151**, 123-131 (2014). <https://doi.org/10.1111/hrd2.00077>  
501 7 Schulte, D. *et al.* The international barley sequencing consortium--at the threshold of  
502 efficient access to the barley genome. *Plant Physiol* **149**, 142-147 (2009).  
503 <https://doi.org/10.1104/pp.108.128967>  
504 8 Jayakodi, M. *et al.* The barley pan-genome reveals the hidden legacy of mutation  
505 breeding. *Nature* **588**, 284-289 (2020). <https://doi.org/10.1038/s41586-020-2947-8>  
506 9 Mascher, M. *et al.* Long-read sequence assembly: a technical evaluation in barley.  
507 *Plant Cell* (2021). <https://doi.org/10.1093/plcell/koab077>  
508 10 Russell, J. *et al.* Exome sequencing of geographically diverse barley landraces and  
509 wild relatives gives insights into environmental adaptation. *Nat Genet* **48**, 1024-1030  
510 (2016). <https://doi.org/10.1038/ng.3612>  
511 11 Druka, A. *et al.* Genetic Dissection of Barley Morphology and Development. *Plant*  
512 *Physiology* **155**, 617-627 (2011). <https://doi.org/10.1104/pp.110.166249>

- 513 12 Wenger, A. M. *et al.* Accurate circular consensus long-read sequencing improves  
514 variant detection and assembly of a human genome. *Nature Biotechnology* **37**, 1155-  
515 1162 (2019). <https://doi.org/10.1038/s41587-019-0217-9>
- 516 13 Padmarasu, S., Himmelbach, A., Mascher, M. & Stein, N. In Situ Hi-C for Plants: An  
517 Improved Method to Detect Long-Range Chromatin Interactions. *Methods Mol Biol*  
518 **1933**, 441-472 (2019). [https://doi.org/10.1007/978-1-4939-9045-0\\_28](https://doi.org/10.1007/978-1-4939-9045-0_28)
- 519 14 Lawniczak, M. K. N. *et al.* Standards recommendations for the Earth BioGenome  
520 Project. *Proceedings of the National Academy of Sciences* **119**, e2115639118 (2022).  
521 <https://doi.org/doi:10.1073/pnas.2115639118>
- 522 15 Maurer, A. *et al.* Modelling the genetic architecture of flowering time control in  
523 barley through nested association mapping. *BMC Genomics* **16**, 290 (2015).  
524 <https://doi.org/10.1186/s12864-015-1459-7>
- 525 16 Li, H., Feng, X. & Chu, C. The design and construction of reference pangenome graphs  
526 with minigraph. *Genome Biology* **21**, 265 (2020). <https://doi.org/10.1186/s13059-020-02168-z>
- 528 17 Andreade, F., Lechat, P., Dufresne, Y. & Chikhi, R. Construction and representation of  
529 human pangenome graphs. *bioRxiv*, 2023.2006.2002.542089 (2023).  
530 <https://doi.org/10.1101/2023.06.02.542089>
- 531 18 De Coster, W., Weissensteiner, M. H. & Sedlazeck, F. J. Towards population-scale long-  
532 read sequencing. *Nature Reviews Genetics* **22**, 572-587 (2021).  
533 <https://doi.org/10.1038/s41576-021-00367-3>
- 534 19 Michelmore, R. W. & Meyers, B. C. Clusters of resistance genes in plants evolve by  
535 divergent selection and a birth-and-death process. *Genome Res* **8**, 1113-1130 (1998).  
536 <https://doi.org/10.1101/gr.8.11.1113>
- 537 20 Wei, F., Wing, R. A. & Wise, R. P. Genome Dynamics and Evolution of the  
538 *Mla* (Powdery Mildew) Resistance Locus in Barley. *The Plant Cell* **14**,  
539 1903-1917 (2002). <https://doi.org/10.1105/tpc.002238>
- 540 21 Bettgenhaeuser, J. *et al.* The barley immune receptor *Mla* recognizes multiple  
541 pathogens and contributes to host range dynamics. *Nature Communications* **12**, 6915  
542 (2021). <https://doi.org/10.1038/s41467-021-27288-3>
- 543 22 Seeholzer, S. *et al.* Diversity at the *Mla* powdery mildew resistance locus from  
544 cultivated barley reveals sites of positive selection. *Mol Plant Microbe Interact* **23**,  
545 497-509 (2010). <https://doi.org/10.1094/mpmi-23-4-0497>
- 546 23 Brabham, H. J. *et al.* Barley *MLA3* recognizes the host-specificity determinant *PWL2*  
547 from rice blast (*M. oryzae*). *bioRxiv*, 2022.2010.2021.512921 (2022).  
548 <https://doi.org/10.1101/2022.10.21.512921>
- 549 24 Rabanus-Wallace, M. T., Wicker, T. & Stein, N. Replicators, genes, and the C-value  
550 enigma: High-quality genome assembly of barley provides direct evidence that self-  
551 replicating DNA forms 'cooperative' associations with genes in arms races. *bioRxiv*,  
552 2023.2010.2001.560391 (2023). <https://doi.org/10.1101/2023.10.01.560391>
- 553 25 Escudero-Martinez, C. M., Morris, J. A., Hedley, P. E. & Bos, J. I. B. Barley  
554 transcriptome analyses upon interaction with different aphid species identify  
555 thionins contributing to resistance. *Plant Cell Environ* **40**, 2628-2643 (2017).  
556 <https://doi.org/10.1111/pce.12979>
- 557 26 Wicker, T., Yahiaoui, N. & Keller, B. Illegitimate recombination is a major evolutionary  
558 mechanism for initiating size variation in plant resistance genes. *The Plant Journal* **51**,  
559 631-641 (2007). [https://doi.org:https://doi.org/10.1111/j.1365-313X.2007.03164.x](https://doi.org/https://doi.org/10.1111/j.1365-313X.2007.03164.x)

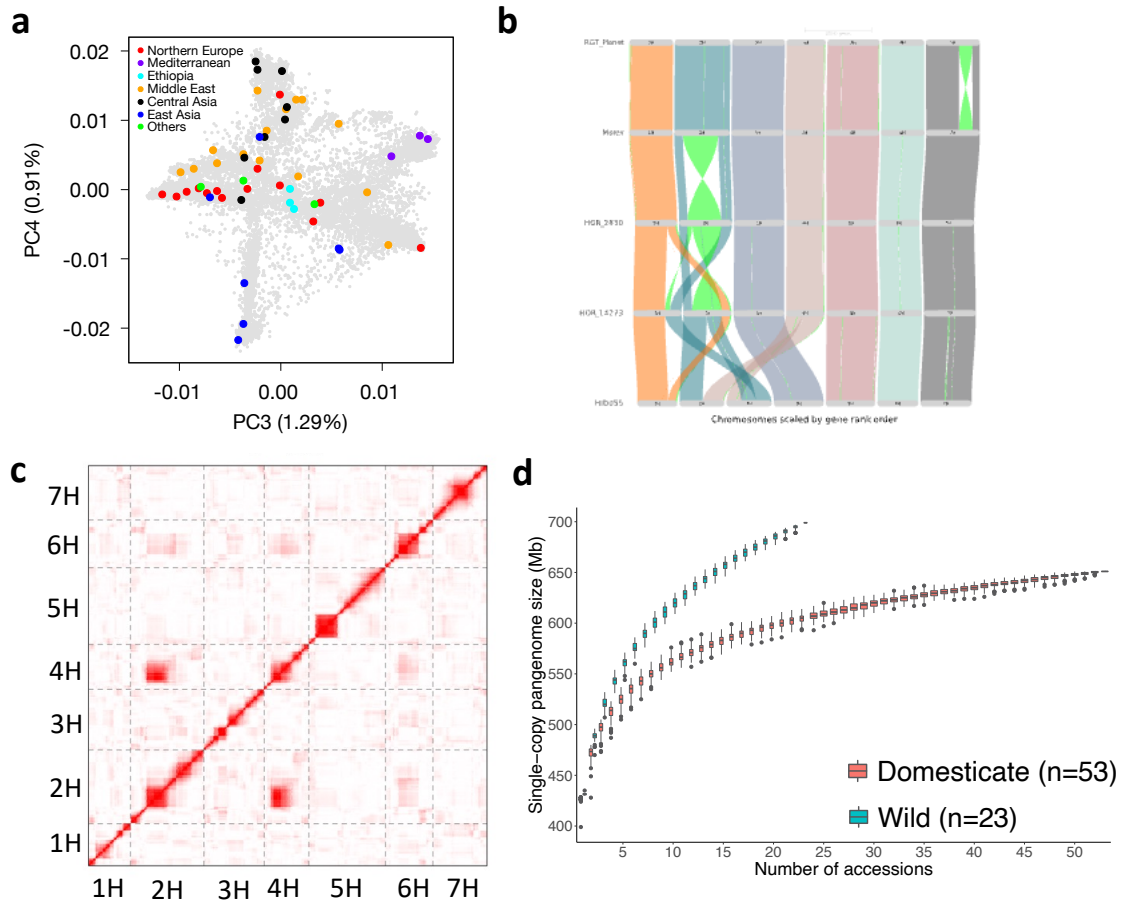
- 560 27 Brassac, J. & Blattner, F. R. Species-Level Phylogeny and Polyploid Relationships in  
561 Hordeum (Poaceae) Inferred by Next-Generation Sequencing and In Silico Cloning of  
562 Multiple Nuclear Loci. *Syst Biol* **64**, 792-808 (2015).  
563 [https://doi.org:10.1093/sysbio/syv035](https://doi.org/10.1093/sysbio/syv035)
- 564 28 Doebley, J., Stec, A. & Hubbard, L. The evolution of apical dominance in maize.  
565 *Nature* **386**, 485-488 (1997). [https://doi.org:10.1038/386485a0](https://doi.org/10.1038/386485a0)
- 566 29 Dixon, L. E. *et al.* TEOSINTE BRANCHED1 Regulates Inflorescence Architecture and  
567 Development in Bread Wheat (*Triticum aestivum*). *The Plant Cell* **30**, 563-581 (2018).  
568 [https://doi.org:10.1105/tpc.17.00961](https://doi.org/10.1105/tpc.17.00961)
- 569 30 Ramsay, L. *et al.* INTERMEDIUM-C, a modifier of lateral spikelet fertility in barley, is  
570 an ortholog of the maize domestication gene TEOSINTE BRANCHED 1. *Nature*  
571 *Genetics* **43**, 169-172 (2011). [https://doi.org:10.1038/ng.745](https://doi.org/10.1038/ng.745)
- 572 31 Lundqvist, U., ABEBE, B. & LUNDQVIST, A. Gene interaction of induced intermedium  
573 mutations of two-row barley. *Hereditas* **111**, 37-47 (1989).  
574 [https://doi.org:10.1111/j.1601-5223.1989.tb00374.x](https://doi.org/10.1111/j.1601-5223.1989.tb00374.x)
- 575 32 Youssef, H. M. *et al.* Natural diversity of inflorescence architecture traces cryptic  
576 domestication genes in barley (*Hordeum vulgare* L.). *Genetic Resources and Crop*  
577 *Evolution* **64**, 843-853 (2017). [https://doi.org:10.1007/s10722-017-0504-6](https://doi.org/10.1007/s10722-017-0504-6)
- 578 33 Monat, C. *et al.* TRITEX: chromosome-scale sequence assembly of Triticeae genomes  
579 with open-source tools. *Genome Biol* **20**, 284 (2019).  
580 [https://doi.org:10.1186/s13059-019-1899-5](https://doi.org/10.1186/s13059-019-1899-5)
- 581 34 Janeček, Š., Svensson, B. & MacGregor, E. A.  $\alpha$ -Amylase: an enzyme specificity found  
582 in various families of glycoside hydrolases. *Cell Mol Life Sci* **71**, 1149-1170 (2014).  
583 [https://doi.org:10.1007/s00018-013-1388-z](https://doi.org/10.1007/s00018-013-1388-z)
- 584 35 Karrer, E. E., Chandler, J. M., Foolad, M. R. & Rodriguez, R. L. Correlation between  $\alpha$ -  
585 amylase gene expression and seedling vigor in rice. *Euphytica* **66**, 163-169 (1992).  
586 [https://doi.org:10.1007/BF00025299](https://doi.org/10.1007/BF00025299)
- 587 36 Mascher, M. *et al.* A chromosome conformation capture ordered sequence of the  
588 barley genome. *Nature* **544**, 427-433 (2017). [https://doi.org:10.1038/nature22043](https://doi.org/10.1038/nature22043)
- 589 37 Kadziola, A., Sogaard, M., Svensson, B. & Haser, R. Molecular structure of a barley  $\alpha$ -  
590 amylase-inhibitor complex: implications for starch binding and catalysis  
591 Edited by R. Huber. *Journal of Molecular Biology* **278**, 205-217 (1998).  
592 [https://doi.org:https://doi.org/10.1006/jmbi.1998.1683](https://doi.org/https://doi.org/10.1006/jmbi.1998.1683)
- 593 38 Zou, X., Neuman, D. & Shen, Q. J. Interactions of two transcriptional repressors and  
594 two transcriptional activators in modulating gibberellin signaling in aleurone cells.  
595 *Plant Physiol* **148**, 176-186 (2008). [https://doi.org:10.1104/pp.108.123653](https://doi.org/10.1104/pp.108.123653)
- 596 39 Fuller, D. Q. Contrasting Patterns in Crop Domestication and Domestication Rates:  
597 Recent Archaeobotanical Insights from the Old World. *Annals of Botany* **100**, 903-924  
598 (2007). [https://doi.org:10.1093/aob/mcm048](https://doi.org/10.1093/aob/mcm048)
- 599 40 Sakuma, S. & Koppolu, R. Form follows function in Triticeae inflorescences. *Breed Sci*  
600 **73**, 46-56 (2023). [https://doi.org:10.1270/jsbbs.22085](https://doi.org/10.1270/jsbbs.22085)
- 601 41 Yu, J. K. & Chung, Y. S. Plant Variety Protection: Current Practices and Insights. *Genes*  
602 (*Basel*) **12** (2021). [https://doi.org:10.3390/genes12081127](https://doi.org/10.3390/genes12081127)
- 603 42 Engledow, F. Inheritance in barley: I. The lateral florets and the rachilla. *Journal of*  
604 *Genetics* **10**, 93-108 (1920).

- 605 43 Cockram, J. *et al.* Genome-wide association mapping to candidate polymorphism  
606 resolution in the unsequenced barley genome. *Proceedings of the National Academy*  
607 *of Sciences* **107**, 21611-21616 (2010). <https://doi.org/doi:10.1073/pnas.1010179107>  
608 44 Beier, S. *et al.* Construction of a map-based reference genome sequence for barley,  
609 *Hordeum vulgare* L. *Scientific Data* **4**, 170044 (2017).  
610 <https://doi.org:10.1038/sdata.2017.44>  
611 45 Kumar, N. *et al.* Functional Conservation in the SIAMESE-RELATED Family of Cyclin-  
612 Dependent Kinase Inhibitors in Land Plants. *Plant Cell* **27**, 3065-3080 (2015).  
613 <https://doi.org:10.1105/tpc.15.00489>  
614 46 Wang, K. *et al.* The CDK Inhibitor SIAMESE Targets Both CDKA;1 and CDKB1  
615 Complexes to Establish Endoreplication in Trichomes. *Plant Physiol* **184**, 165-175  
616 (2020). <https://doi.org:10.1104/pp.20.00271>  
617 47 Knudsen, S. *et al.* FIND-IT: Accelerated trait development for a green evolution.  
618 *Science Advances* **8**, eabq2266 (2022). <https://doi.org:doi:10.1126/sciadv.abq2266>  
619 48 Nomoto, Y. *et al.* A hierarchical transcriptional network activates specific CDK  
620 inhibitors that regulate G2 to control cell size and number in Arabidopsis. *Nature*  
621 *Communications* **13**, 1660 (2022). <https://doi.org:10.1038/s41467-022-29316-2>  
622 49 Liao, W.-W. *et al.* A draft human pangenome reference. *Nature* **617**, 312-324 (2023).  
623 <https://doi.org:10.1038/s41586-023-05896-x>  
624 50 Brown, T. A. Is the domestication bottleneck a myth? *Nature Plants* **5**, 337-338  
625 (2019). <https://doi.org:10.1038/s41477-019-0404-1>  
626  
627



628 **Figures**

629



630

631

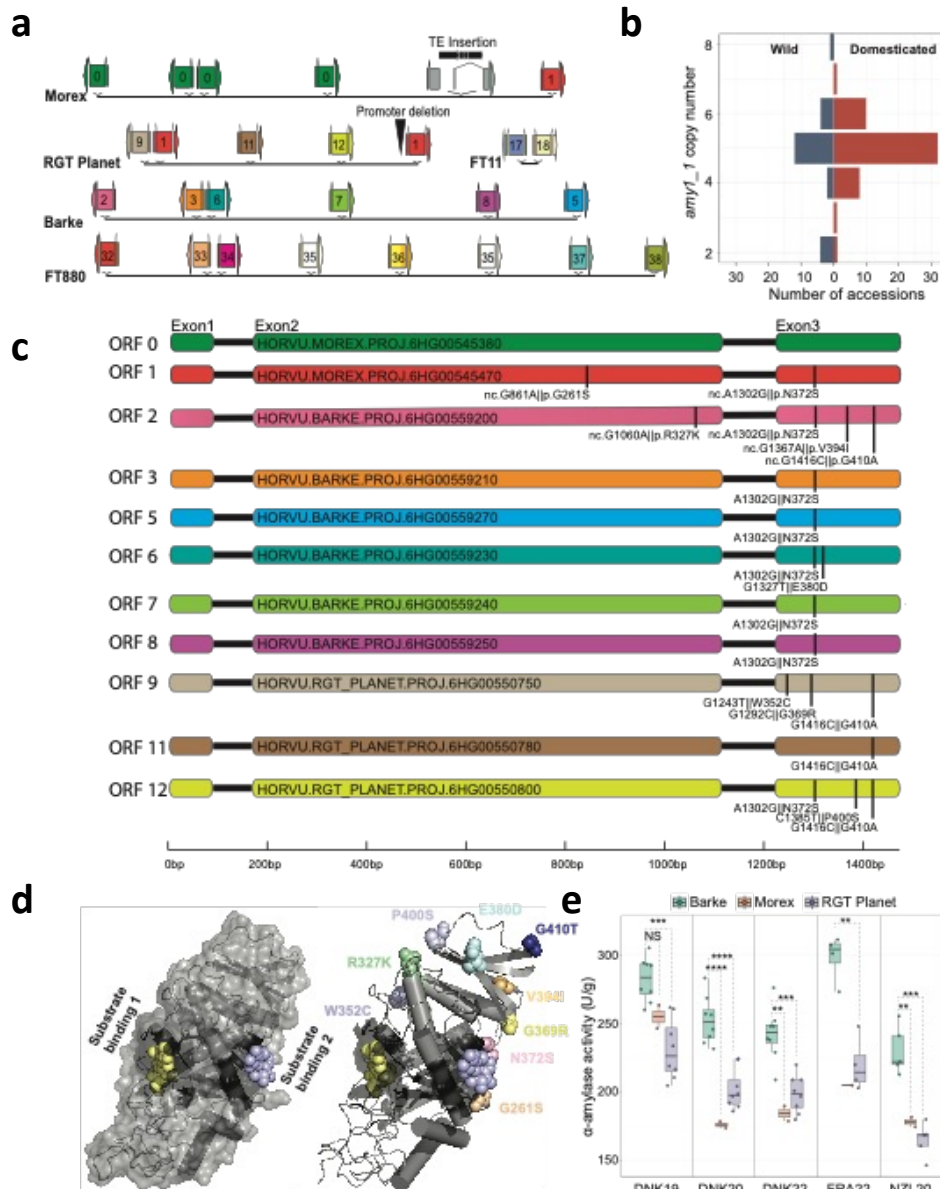
632 **Figure 1:** A species-wide pangenome of *Hordeum vulgare*. (a) Principal component analysis  
633 showing domesticated accessions (n=53) in the pangenome panel in the global diversity  
634 space. Regions of origins are color coded. The proportion of variance explained by each PC in  
635 panels is given in the axis labels. Other PCs are shown in **Extended Data Fig. 1a**. (b) Example  
636 of large structural variants including interchromosomal translocations and inversions  
637 between pangenome accessions. (c) Interchromosomal linkage disequilibrium (LD) in  
638 segregating offspring derived from a cross between HID055 and Barke. LD is indicated by the  
639 intensity of red color. (d) Size of the single-copy pangenome in wild and domesticated  
640 barleys as a function of sample size.

641

642

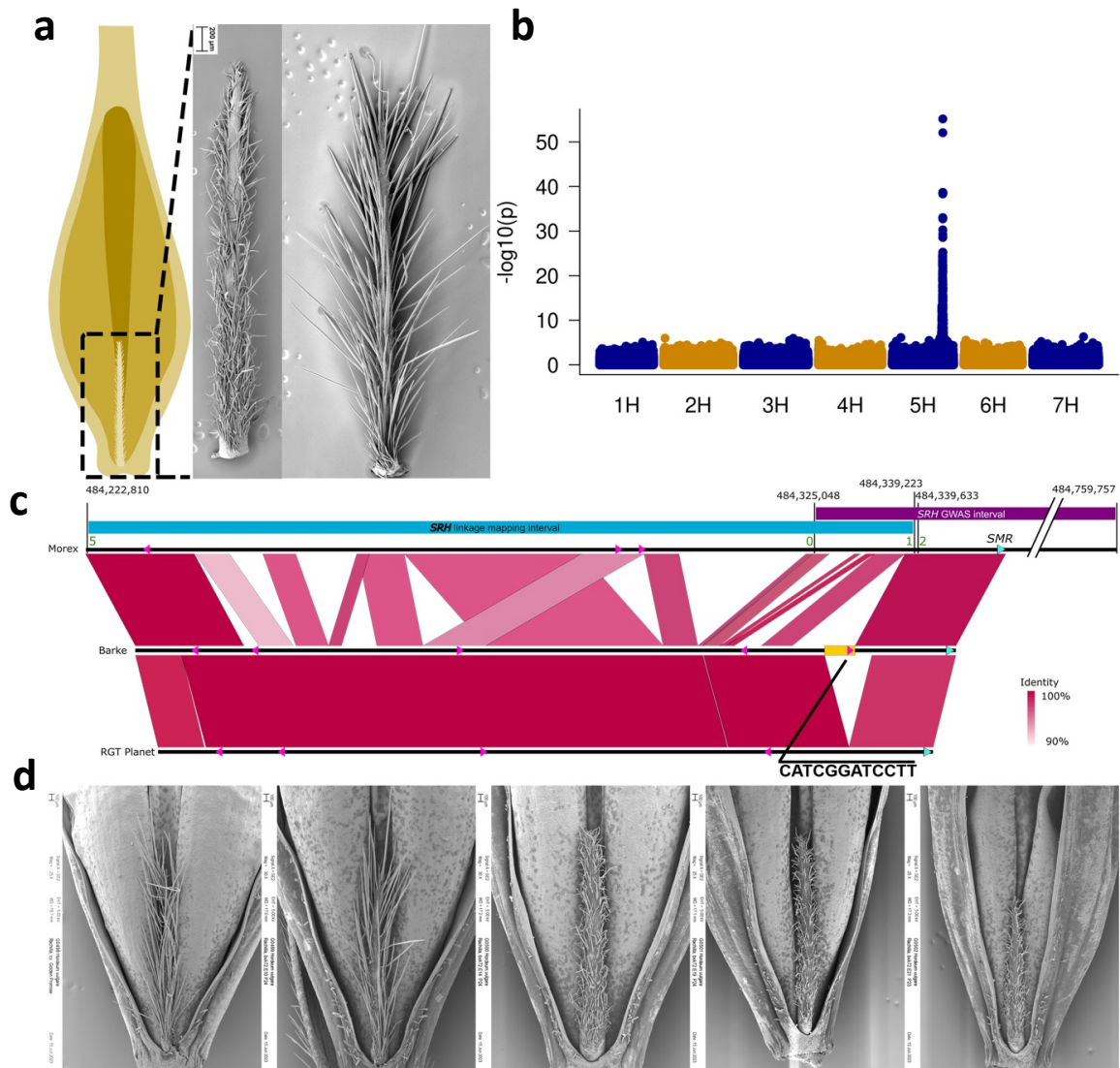






663  
664

665 **Figure 3. Structural diversity at the *amy1\_1* locus and its importance in malting. (a)**  
666 Simplified structure of the *amy1\_1* locus in selected pangenome assemblies. A detailed  
667 depiction of the *amy1\_1* locus across all 76 assemblies is shown in **Extended Data Fig. 9a**.  
668 Identical ORFs have the same colours in **(a)** and **(c)**. **(b)** Distribution of *amy1\_1* copy numbers  
669 in wild and domesticated accessions of the pangenome. **(c)** Non-synonymous sequence  
670 exchanges in 12 non-redundant *amy1\_1* ORFs in the malting barleys Morex, Barke and RGT  
671 Planet. The positions of sequence variants and respective amino acid variations are marked  
672 by black lines. ORF numbers refer to **Supplementary Table 13**. **(d,e)** X-ray crystal structure  
673 (pdb: 1BG9; ref. <sup>36</sup>) of  $\alpha$ -amylase bound to acarbose as a substrate analogue (magenta and  
674 yellow spheres in panel **(d)**). In panel **(e)**, *amy1\_1* amino acid variants (found in Morex, Barke  
675 and RGT Planet, **Supplementary Table 20**) are added as coloured spheres. **(f)**  $\alpha$ -amylase  
676 activity of micro-malted near-isogenic lines (NILs) containing *amy1\_1*-Morex, Barke and RGT  
677 Planet haplotypes.  
678



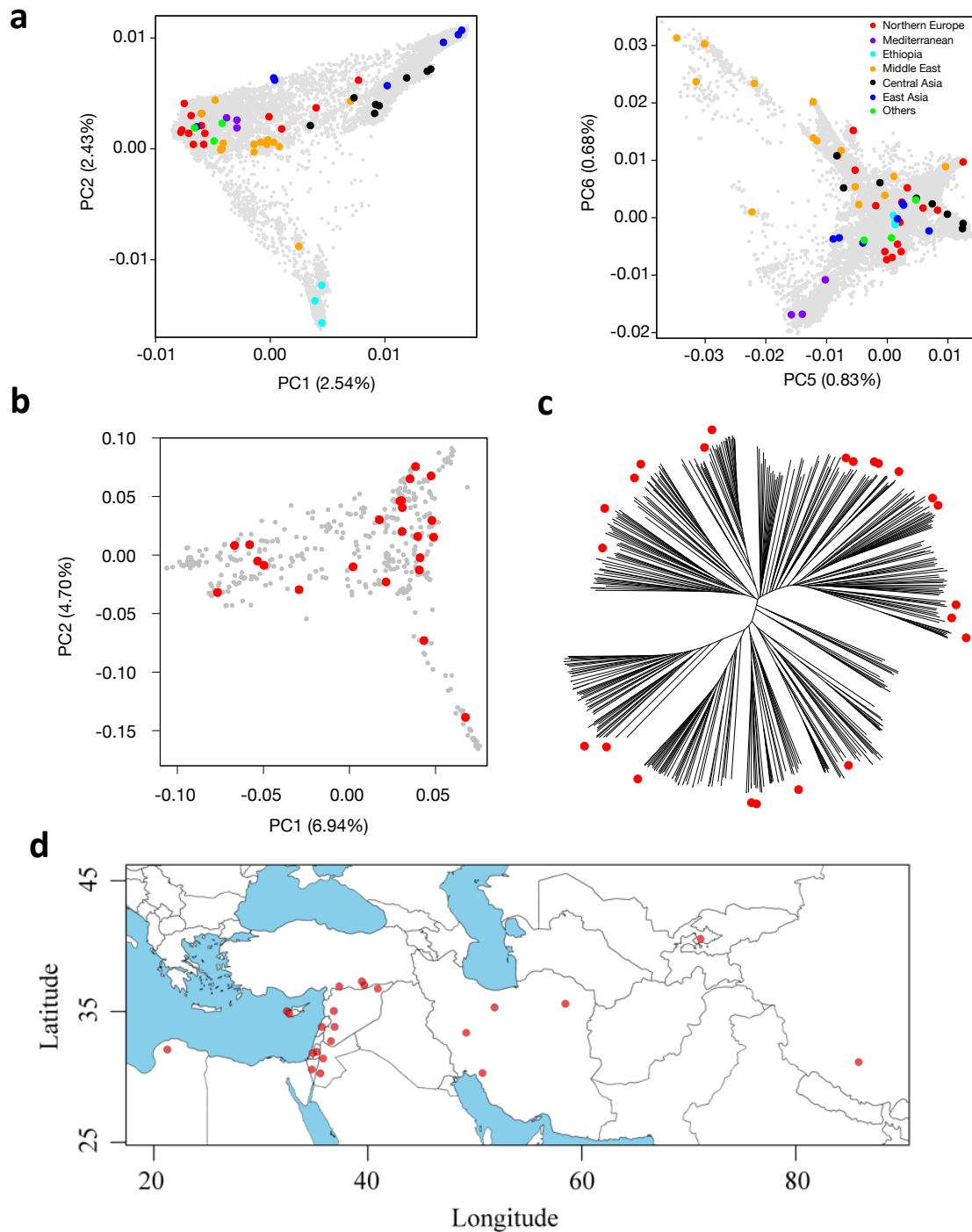
679

680

681 **Figure 4. A deletion in an enhancer motif is associated with trichome branching. (a)**  
682 Schematic drawing of a seed from a hulled and awned barley. The rachilla is a rudimentary  
683 structure attached to the base of the seed, representing reduced lateral branches in the  
684 barley inflorescence. On the right, scanning electron micrographs are shown of a short-  
685 haired and a long-haired rachilla of genotypes Morex and Barke, respectively. **(b)** Genome-  
686 wide association study (GWAS) for rachilla hair phenotype in the core1000. **(c)** Top part:  
687 schematic representation of the high-resolution genetic linkage analysis at the *Srh1* locus.  
688 Blue and purple horizontal bars represent the overlapping biparental and GWAS mapping  
689 intervals in reference to the 160 kb physical interval in the Morex genome (black line below  
690 the colored bars). Note, the SMR-like gene sits outside the high-resolution biparental  
691 mapping interval. Bottom part: connector plot showing orthologous regions in the  
692 genotypes Barke (long hairs) and RGT Planet (short hairs). A region harboring a conserved  
693 enhancer element (yellow rectangle) is present in Barke, but absent in Morex and RGT  
694 Planet. **(d)** Rachilla hair phenotype of the Cas9-induced knock-out mutants of the SMR-like  
695 gene. From left to right: wild-type Golden Promise (GP); wild-type segregant from the  
696 brhE72P19 family; independent mutant segregants showing the short-hair phenotype.  
697

698 **Extended Data Figures**

699



700

701

702 **Extended Data Figure 1: A globally representative diversity panel of domesticated and wild**

703 **barley. (a)** Higher principal components (PC) of the barley diversity space with pangenome

704 accessions highlighted. **(b)** The first two PCs of the diversity space of 412 wild barley

705 (*Hordeum vulgare* subsp. *spontaneum*) with pangenome accessions highlighted. **(c)**

706 Neighbor-joining phylogenetic tree of those wild barleys. The branch tips corresponding to

707 accessions selected for the pangenome are marked with red circles. The proportion of

708 variance explained by each PC in panels **(a)** and **(b)** is given in the axis labels. **(d)** Map

709 showing the collection sites of wild accessions (n=23) included in the pangenome panel.

**a**

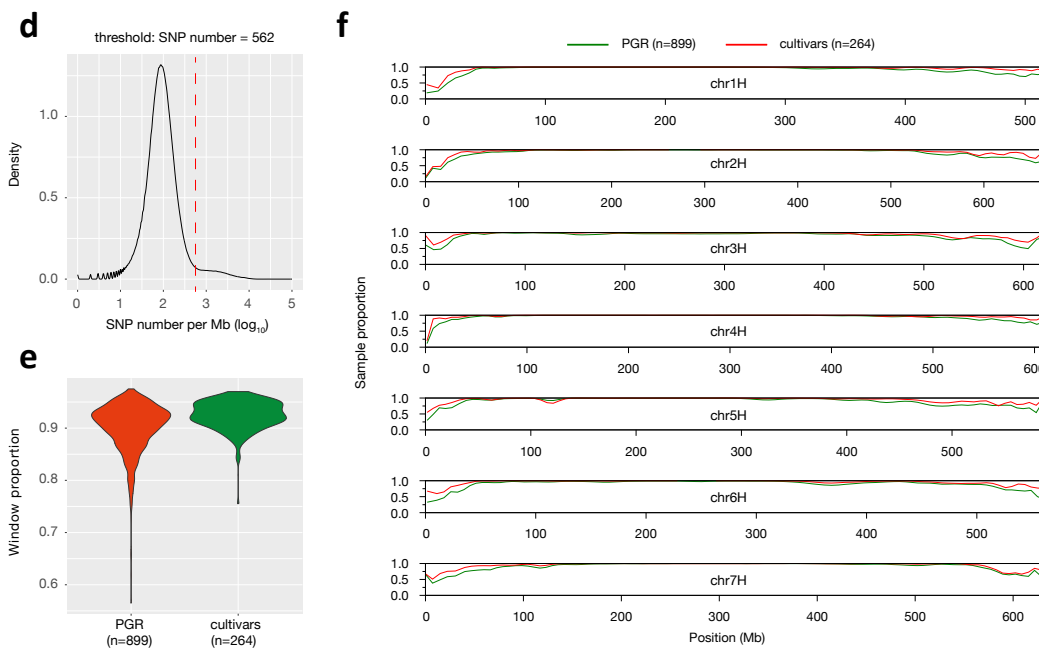
Quality category	Metric	Domesticate (N=53)	Wild (N=23)
Continuity	Avg. contig N50	18	14
	Max. contig N50	37	21
	Min. contig N50	10	8
	Avg. no. of gaps	445	556
Chromosome status	Avg. chromosome anchoring rate (%)	98.0	98.1
	Avg. chromosome anchored size (Gb) unanchored size (Mb)	4.19 47	4.21 53
Structural accuracy	False duplications (%)	0.012	0.010
	Curation (Hi-C)	Manual	Manual
Base accuracy	Consensus quality value (QV)	66.0	66.3
	k-mer completeness (%)	97.5	97.6
Functional completeness	BUSCO (%)	96.4	96.5

**b**

	Summary
No. of PAVs (> 50 nt)	1,703,288
Presence in Morex	787,285
Absence in Morex	916,003
Polymorphic (>2 & < 74)	581,248 (34%)

**c**

Type	Summary
Inversions (> 2 kb)	3,277
Shared events (>2 & < 74)	548 (17%)
Private to domesticate	197
Private to wild	76

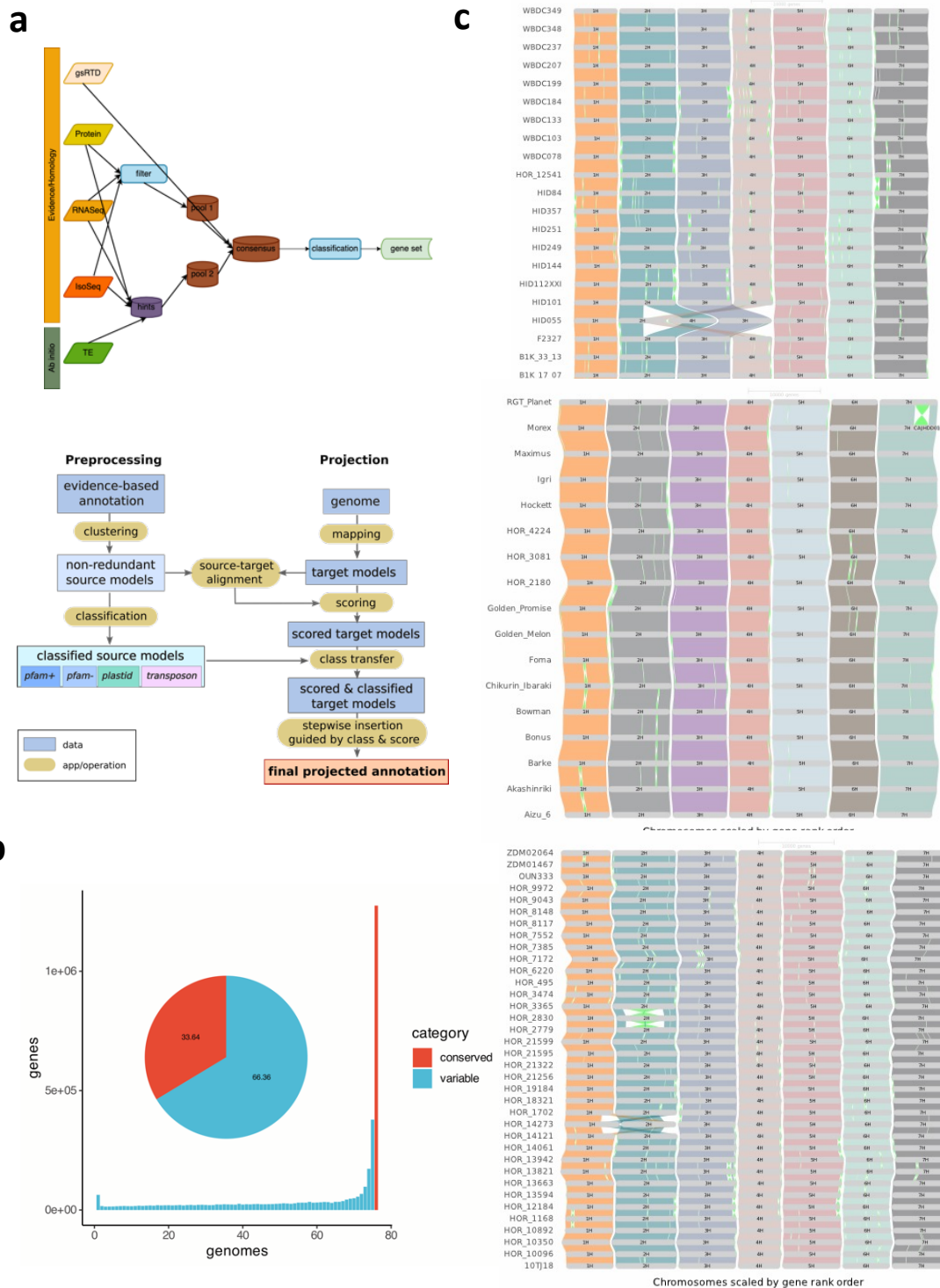


709  
710  
711  
712  
713  
714  
715  
716  
717

**Extended Data Figure 2: A pangenomic diversity map of barley. (a)** Assembly statistics of 76 chromosome-scale reference genomes sequences. **(b)** Counts of presence/absence variants. **(c)** Counts of inversion polymorphisms spanning 2 kb or more. **(d)** Selection of threshold based on pairwise differences (number of SNPs per Mb) for the binary classification into similar/dissimilar haplotypes. **(f)** The proportion of samples with a close match to one of the 76 pangenome accessions is shown for plant genetic resources (PGR) and elite cultivars in sliding windows along the genome (size: 1 Mb, shift: 500 kb). **(h)** Distribution of the share of similar windows in individual PGR and cultivar genomes.



718



719  
720

721 **Extended Data Figure 3: Gene annotation and orthologous framework.** (a) Workflow for  
722 annotating, projecting and clustering gene models. The upper panel describes the workflow  
723 for the de-novo gene predictions, the lower panel for the gene projections (b) Histogram  
724 showing the number of pagenome genotypes contributing to individual hierarchical  
725 orthologous groups (HOGs). The pie chart shows the ratio between conserved and variable  
726 genes. (c) GENESPACES alignments of 76 barley genomes, grouped by wild barley, cultivated  
727 barley and landraces.



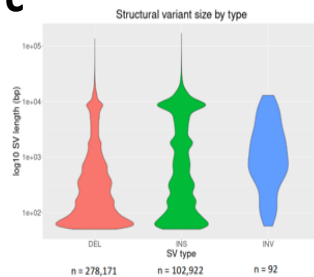
**a**

chromosome	# nodes	# edges	combined node length (bp)
chr1H	615,439	874,894	1,092,683,108
chr2H	789,027	1,123,085	1,409,260,038
chr3H	778,830	1,106,625	1,332,024,267
chr4H	627,447	890,321	1,094,625,160
chr5H	719,146	1,024,533	1,295,813,787
chr6H	677,475	963,220	1,174,448,066
chr7H	848,394	1,206,148	1,442,759,314
joint graph	5,055,758	7,188,826	8,841,613,740

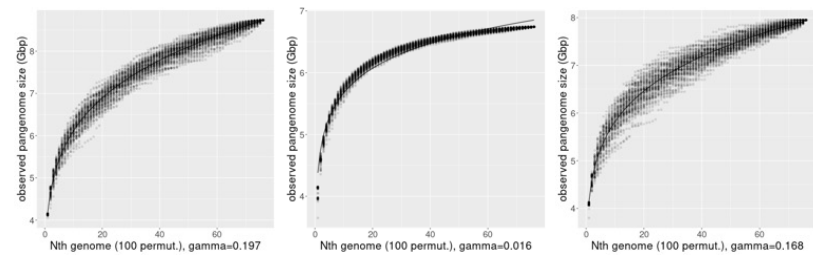
**b**

accession	mapping to graph	mapping to linear reference	difference (linear - graph)
% reads mapped			
ERR2766176	97.25	98.42	1.17
SRR10200200	98.62	99.81	1.19
SRR5197485	97.19	99.7	2.51
SRR5197496	97.15	99.71	2.56
SRR6281633	93.15	95.66	2.51
% reads properly paired			
ERR2766176	96.54	92.52	-4.02
SRR10200200	96.47	94.03	-2.44
SRR5197485	94.7	93.81	-0.9
SRR5197496	94.46	94.74	0.28
SRR6281633	92.08	90.47	-1.61
% mismatches			
ERR2766176	1.16	1.4	0.24
SRR10200200	1.08	1.28	0.2
SRR5197485	0.83	0.92	0.09
SRR5197496	0.79	0.89	0.1
SRR6281633	1.5	1.73	0.23
# mismatches			
ERR2766176	578,805,187	711,908,069	133,102,882
SRR10200200	1,011,740,607	1,212,059,305	200,318,698
SRR5197485	581,657,638	666,287,736	84,630,098
SRR5197496	569,171,755	656,634,935	87,463,180
SRR6281633	1,496,337,825	1,767,306,648	270,968,823

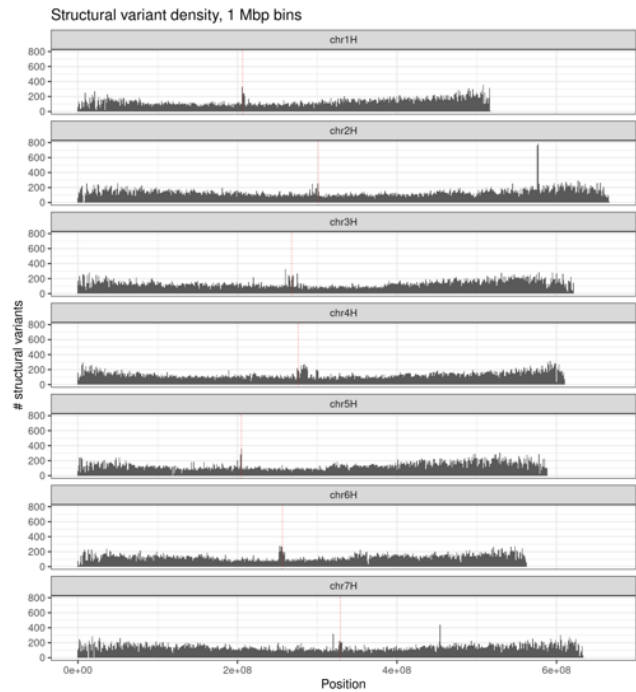
**c**



**e**

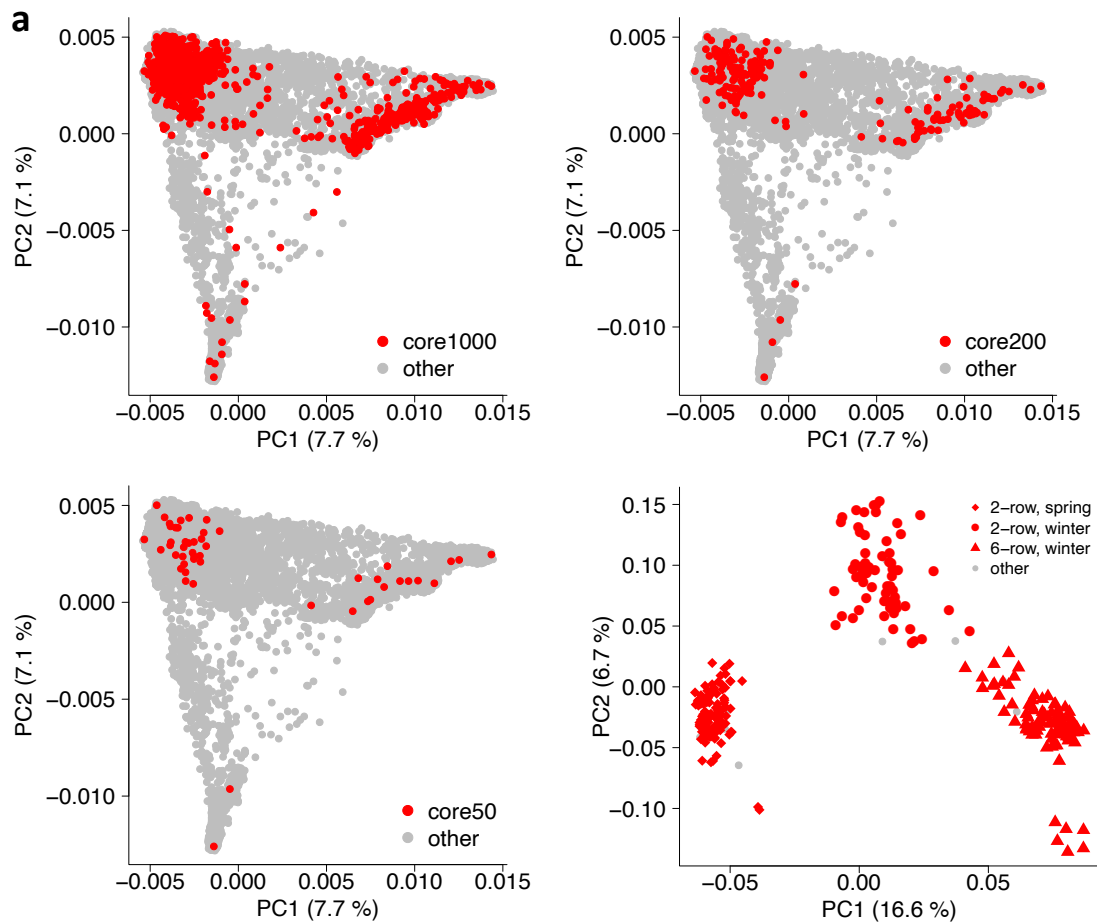


**d**



728  
729

730 **Extended Data Figure 4:** Graph-based pan-genome analysis with Minigraph. **(a)** Descriptive  
731 statistics per chromosome and for joint graph. **(b)** Comparative statistics of read mappings  
732 from five publicly available Illumina whole genome shotgun sequence read runs against the  
733 pan-genome graph and the MorexV3 linear reference sequence. **(c)** Size distribution of  
734 structural variants (SVs) in graph. **(d)** Chromosomal distribution of SVs. Centromere positions  
735 are indicated by vertical dashed lines in red. **(e)** Pan-genome graph growth curves generated  
736 with the odgi heaps tool. One hundred permutations were computed for each number of  
737 genomes included. Values of gamma > 0 in Heaps' law indicate an open pan-genome. Plots  
738 shown are for all accessions (left, n = 76), domesticated accessions only (cultivars +  
739 landraces, centre, n = 53) and *H. spontaneum* accessions (right, n = 23).  
740



**b**

Chromosome	SNPs	indels
chr1H	17,314,288	1,088,174
chr2H	24,995,054	1,569,302
chr3H	24,482,473	1,695,142
chr4H	20,039,734	1,372,443
chr5H	21,590,485	1,411,261
chr6H	22,929,086	1,477,914
chr7H	24,207,458	1,603,509
<b>Total</b>	<b>155,558,578</b>	<b>9,129,571</b>

741

742

743 **Extended Data Figure 5: Short-read data complement the pangenome infrastructure. (a)**

744 Accessions selected for short-read sequencing. Nested coresets of 1000, 200 and 50

745 accessions (core1000, core200, core50) are shown in the global diversity space of barley as

746 represented by a principal component (PCA). The top-right subpanel shows a PCA of 315

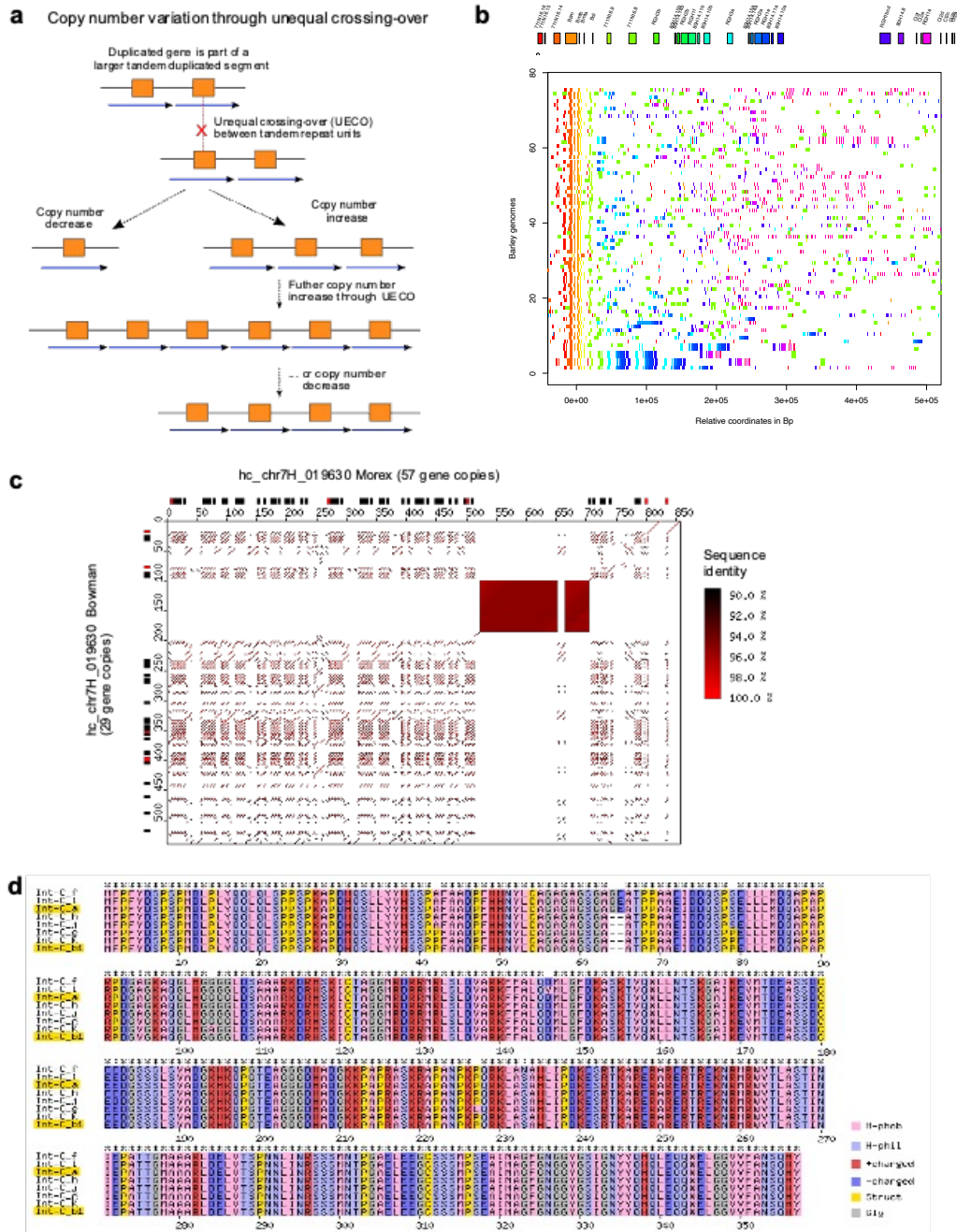
747 elite cultivars. Accessions are according to genepool (2-rowed spring, 2-rowed winter, 6-

748 rowed winter). The proportion of variance explained by the PCA is shown in the axis labels.

749 **(b)** Counts of single-nucleotide polymorphisms (SNPs) and short insertions and deletions

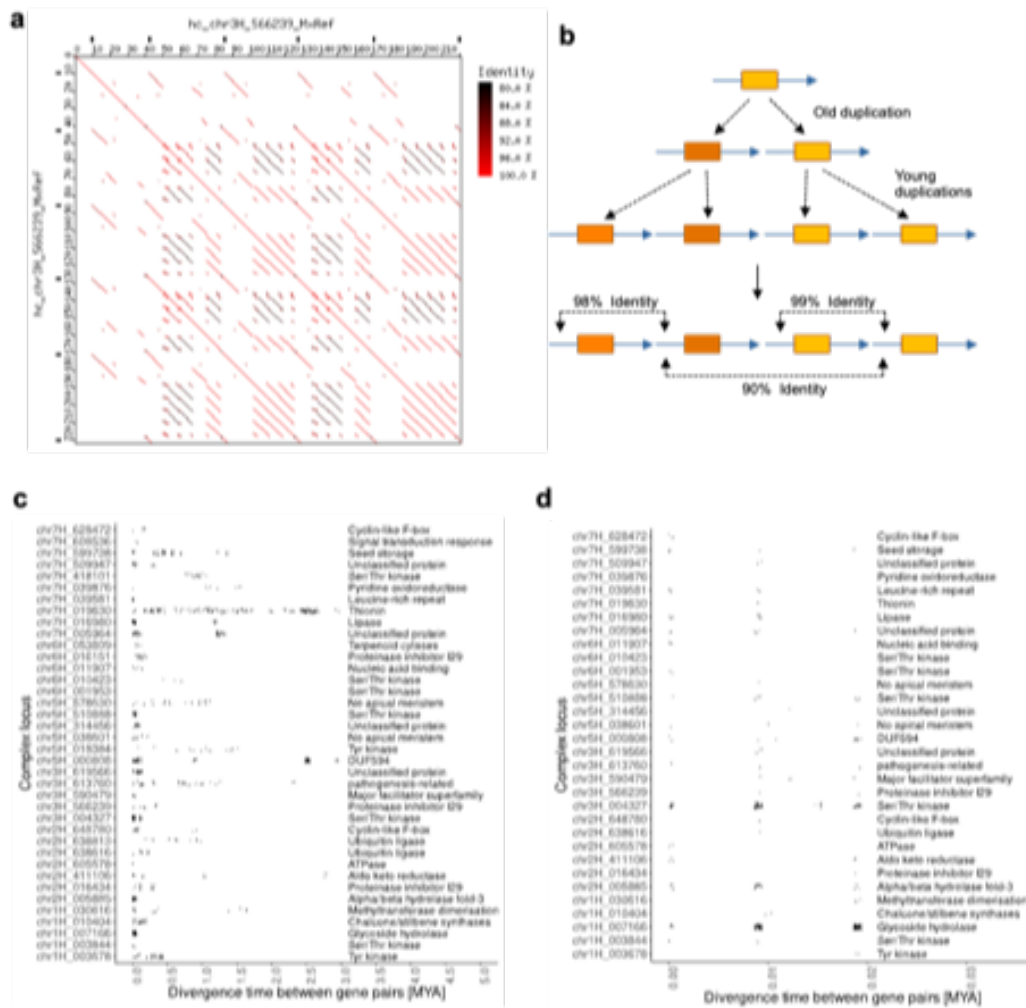
750 (indels) detected in those data.

751



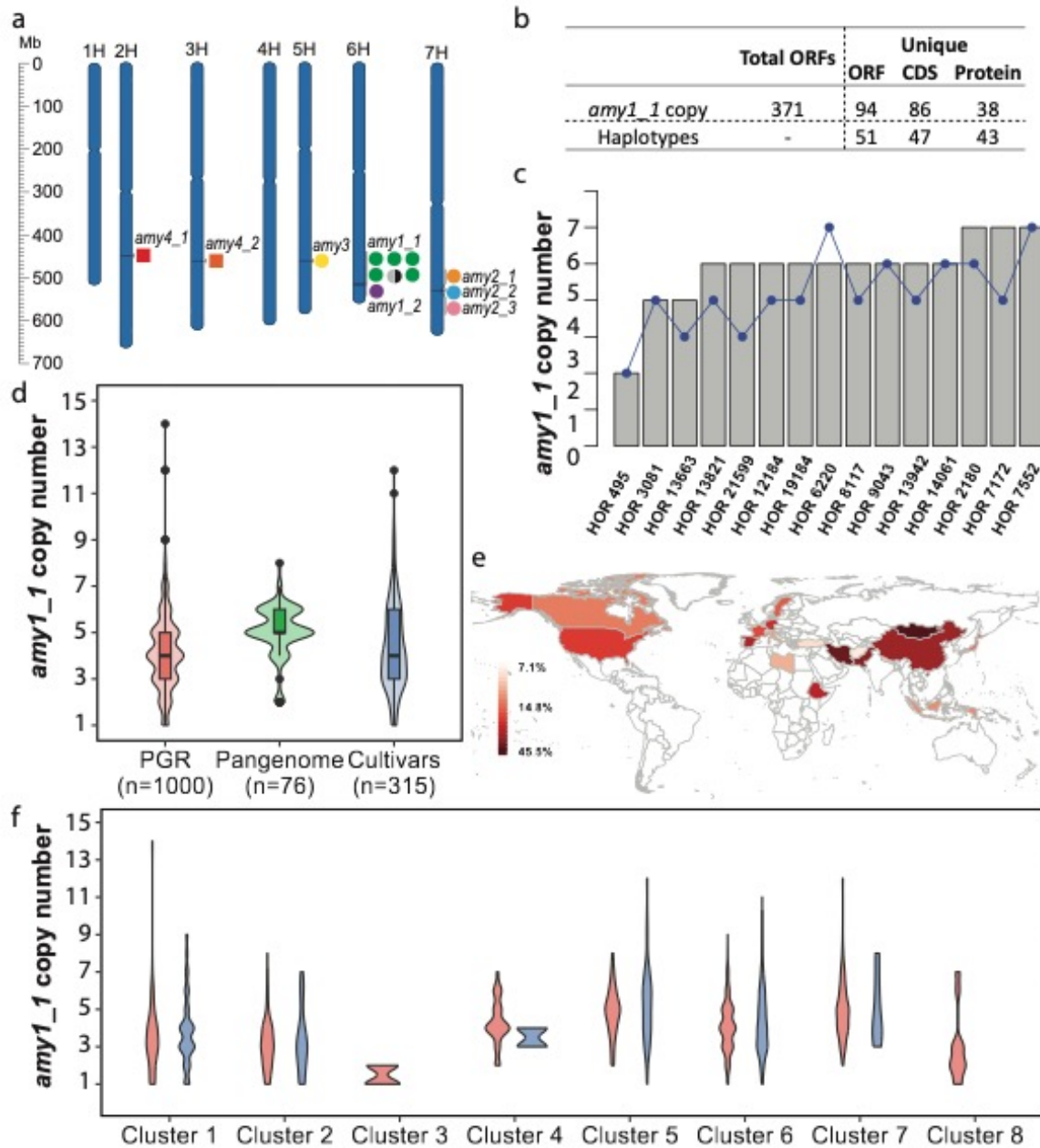
752  
753

754 **Extended Data Figure 6. Complex loci are hot spots for copy number variation (CNV).** (a) The schematic  
755 model shows how, once an initial duplication is established, unequal homologous recombination (unequal  
756 crossing-over, UECO) between repeat units can lead to rapid expansion and contraction of the loci, thereby  
757 leading to CNV of genes. (b) Structure of the *Mla* region across the 76 pangenome accessions. The gene  
758 models present in the Morex genome are shown on top. (c) Dot plot alignment of the example locus  
759 chr7H\_019630 which contains a cluster of thionin genes. The sequences of cv. Morex (horizontal) and wild  
760 barley HID101 (vertical) were aligned. Predicted intact genes are indicated as black boxes along the left and top  
761 axes. Predicted pseudogenes are shown in red. The axis scale is kb. The filled rectangle at positions ~520-720  
762 kb in Morex represents an array of short tandem repeats which does not contain genes and does not have  
763 sequence homology to the gene-containing tandem repeats of the locus. (d). Predicted protein variants of *Int-c*  
764 (*HvTB1*) genes. Previously described alleles are highlighted in yellow. Color code: H-phob: Hydrophobic aa, H-  
765 phil: Hydrophilic aa, +charged: positively charged aa, - charged: negatively charged aa, Struct: structural aa,  
766 Cystein or Prolin, Gly: Glycin.

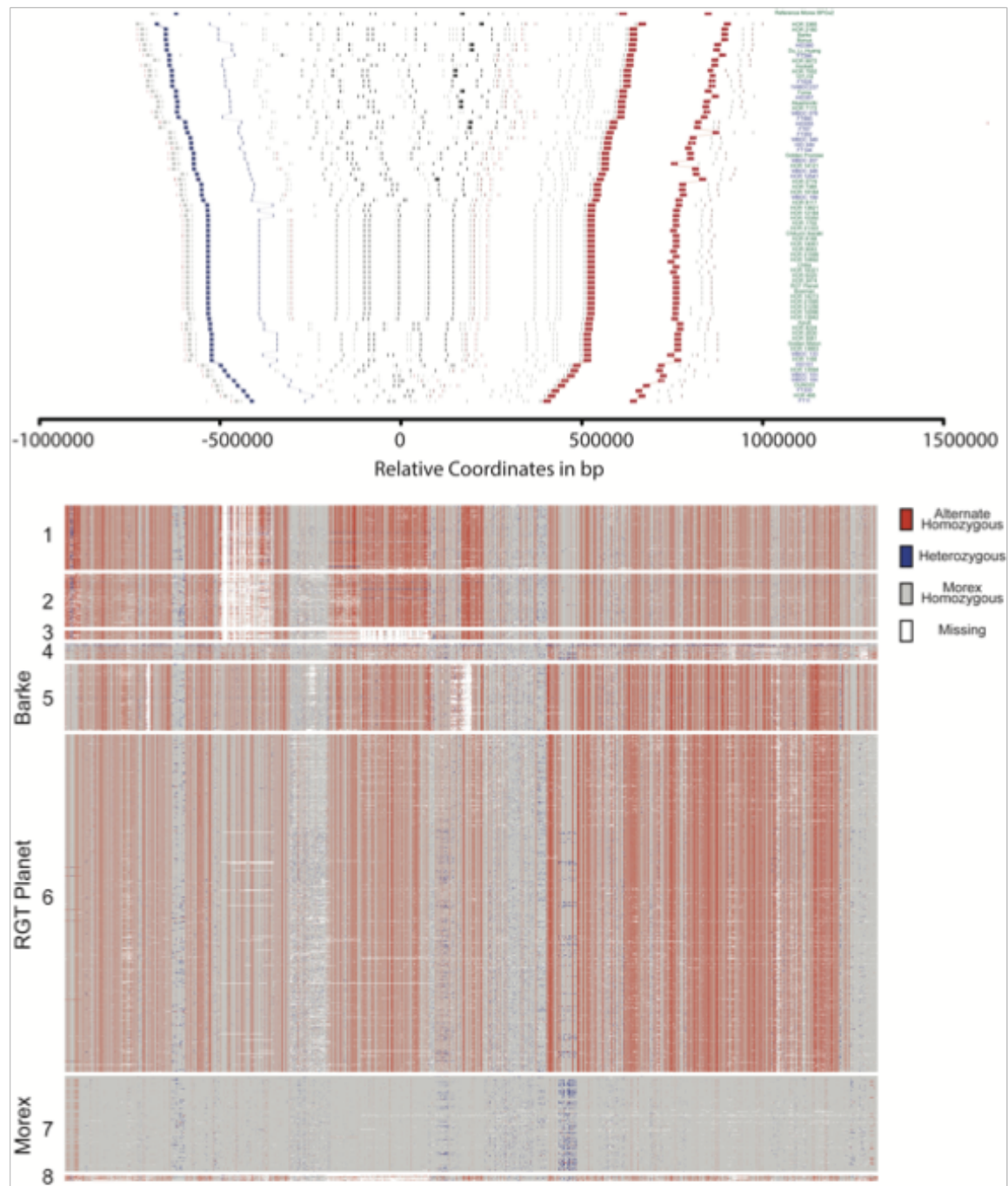


767  
 768 **Extended Data Figure 7.** Molecular dating of divergence times between duplicated gene  
 769 copies in complex loci. **(a)** Dot plot example of locus `hc_chr3H_566239` which underwent  
 770 multiple waves of tandem duplications, which is reflected in varying levels of sequence  
 771 identity between tandem repeats (color-coded). **(b)** Schematic mechanism for how different  
 772 levels of sequence identity between tandem repeats evolve. In the example, an ancestral  
 773 duplication was followed by two independent subsequent duplications, leading to varying  
 774 levels of sequence identity between tandem repeat units. Genes are indicated as orange  
 775 boxes while blue arrows indicate the tandem repeats they are embedded in. **(c)** Divergence  
 776 time estimates between duplicated gene copies in complex loci. Shown are only those  
 777 complex loci which have at least six tandem-duplicated genes. Each dot represents one  
 778 divergence time estimate for a duplicated gene pair from the respective locus. The x-axis  
 779 shows the estimated divergence time in million years. At the right-hand side, classification of  
 780 proteins encoded by genes in the locus are shown. Note that several loci had multiple waves  
 781 of gene duplications over the past 3 million years. **(d)** Subset of those loci shown in (c) that  
 782 had at least one gene duplication within the past 20,000 years. The divergence time  
 783 estimates appear in groups, since they represent the presence of 0, 1 and 2 nucleotide  
 784 substitutions, respectively, in the approx. 4 kb of aligned sequences that were used for  
 785 molecular dating.





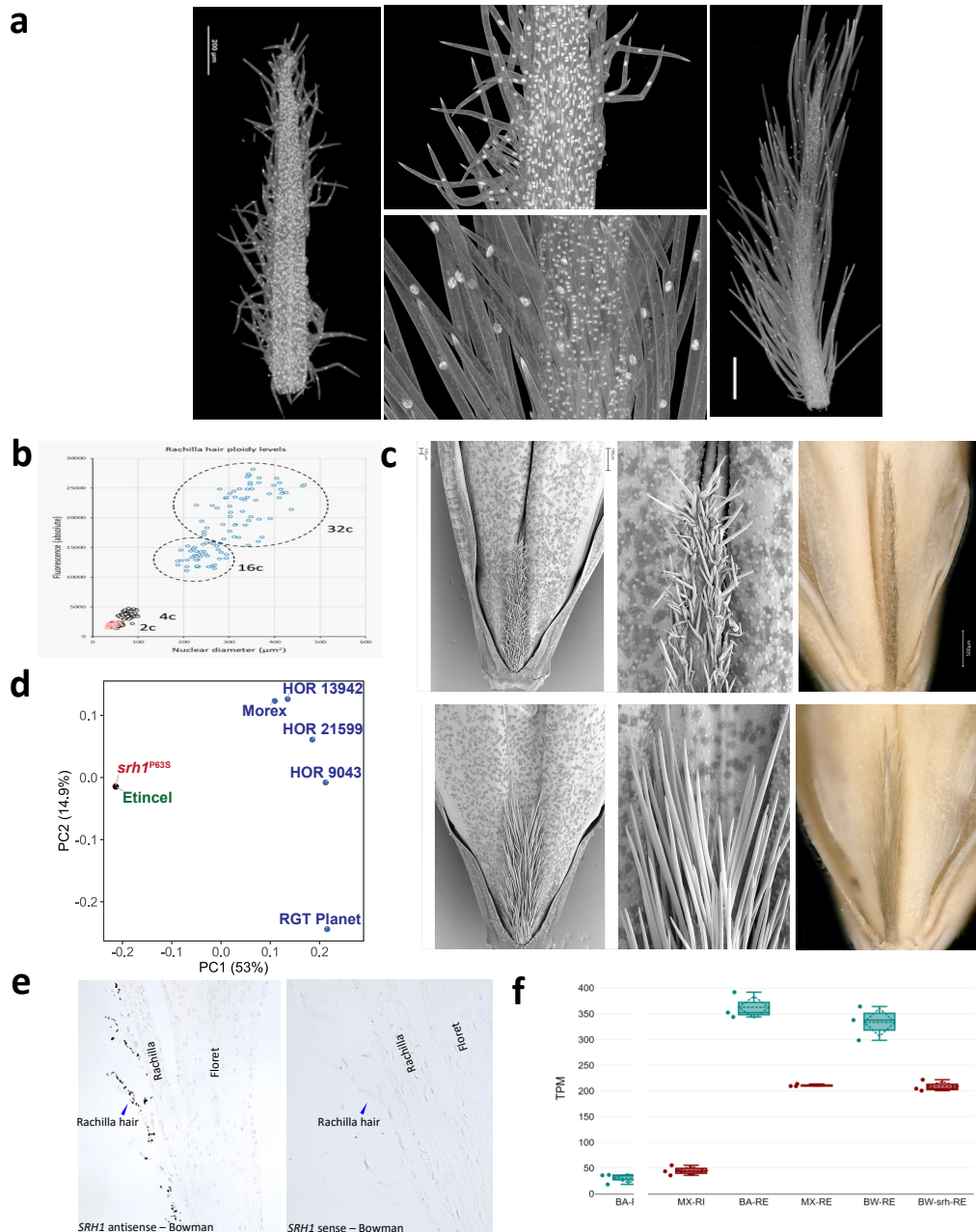
786  
 787 **Extended Data Figure 8. *amy1\_1* locus structure and copy number in 76 assemblies and 1,315**  
 788 **whole genome sequenced accessions. (a)** Chromosomal location of 12  $\alpha$ -amylase genes in the  
 789 MorexV3 genome assembly. **(b)** Summary of *amy1\_1* locus sequence diversity in 76 pangenome  
 790 assemblies (**Supplementary Tables 13-16, 18-19**). Total *amy1\_1* ORFs in pangenome and unique  
 791 copies and haplotypes of ORF, CDS and protein. Haplotype denotes unique combinations of ORF, CDS  
 792 and protein in individual accessions. **(c)** Comparison of *amy1\_1* copy numbers identified in the  
 793 pangenome assemblies versus *k*-mer based estimation from raw reads. Grey bars denote copy  
 794 number from pangenome, blue dots denote *k*-mer estimated copy number. **(d)** *amy1\_1* copy number  
 795 estimation in 76 pangenome assemblies ("Pangenome"), 1,000 whole-genome sequenced plant  
 796 genetic resources ("PGR"), and 315 whole-genome sequenced European elite cultivars ("Cultivars")  
 797 using *k*-mer based methods. **(e)** Distribution of accessions with *amy1\_1* copy numbers >5 per  
 798 country (as percentage of total accessions in country for countries with  $\geq 10$  accessions). **(f)** *amy1\_1*  
 799 copy number within each haplotype cluster (see **Extended Data Figure 9b**). Red color refers to 1,000  
 800 plant genetic resource accessions, green refers to 76 pangenome accessions and blue refers to 315  
 801 European elite cultivars. Cluster #5, #6 and #7 contain Barke, RGT Planet and Morex, respectively.



802  
803  
804  
805  
806  
807  
808  
809  
810  
811  
812  
813  
814

**Extended Data Figure 9. Haplotype structure of the *amy1\_1* locus. (a)** Structural diversity in the vicinity of *amy1\_1* in the 76 pangenome assemblies. Each line shows the gene order in the sequence assembly of one genotype. The Morex V3 reference is shown on top. Coloured rectangles stand for gene models extracted from BLAST alignments against the corresponding gene models in MorexV3. Black rectangles represent *amy1\_1* homologs and grey rectangles other genes. Blue and red rectangles represent marker genes used to define the synteny, delimit the region, and sort the accessions based on the distance between endpoints. Lines connect genes models between different genomes. Accession names are given on the right axis and are coloured according to type (blue – wild, green – domesticated). In HOR 8148, five copies assigned to 6H are shown. Two copies assigned to an unanchored contig are not shown. **(b)** SNP haplotype clusters at the *amy1\_1* locus among 1,315 genomes of domesticated and wild barley accessions, including genomes of 315 elite barley cultivars. The 6H:516,385,490-517,116,415 bp in the Morex V3 genome sequence is shown. Haplotype clusters #5, #6 and #7 contain the elite malting varieties Barke, RGT Planet and Morex, respectively.





815  
 816 **Extended Data Figure 10: Genetic dissection of the *srh1* locus.** (a) Light microscopy of short- and long-haired  
 817 rachillae at developmental stage W8.5-9 using DAPI staining to visualize the nuclei. Size differences of nuclei in  
 818 epidermal and trichome cells are very obvious. (b) Densitometric measurement of DNA content in epidermal and  
 819 trichome cells of DAPI stained rachillae of genotypes Morex and Barke, respectively. While trichome cells  
 820 in short-haired rachillae undergo only one cycle of endoreduplication, the cells in long haired trichomes show  
 821 eight to sixteen-fold higher DNA contents than epidermal cells indicating three to four cycles of  
 822 endoreduplication. (c) *srh1* mutant discovery. FIND-IT screenings identified a mutant with short-fuzzy hairs  
 823 (top) in the background of the long-haired variety Etincel (bottom). The mutants are a P64S non-synonymous  
 824 sequence exchange. Scale bar - 1mm. (d) Principal coordinate analysis of SNP array genotyping data of different  
 825 barley genotypes. Etincel and its mutant cluster together, proving their isogenicity. (e) mRNA *in situ*  
 826 hybridization of *HvSRH1* in longitudinal spikelet sections of Bowman with anti-sense (left) and sense (right)  
 827 probes. The blue arrow indicates the position of a rachilla hair. (f) *HvSRH1* transcript abundance in RNA  
 828 sequencing data of rachilla tissue in Barke (BA, long-haired), Morex (MX, short-haired), Bowman (BW, long-  
 829 haired) and a short-haired near-isogenic line of Bowman (BW-srh). Samples were taken at two development  
 830 stages: rachilla hair initiation (RI) and elongation (RE). Abundance was measured as transcripts per million  
 831 (TPM).



## 833 **Plant growth and high molecular weight DNA isolation**

834

835 Twenty-five seeds each from the selected accessions (**Supplementary Tables 1 and 6**) were  
836 sown on 16 cm diameter pots with compost soil. Plants were grown under greenhouse  
837 conditions with sodium halogen artificial 21°C in the day for 16 hrs and 18°C at night for 8 hrs.  
838 Leaves (8 g) were collected from 7-day old seedlings, ground with liquid nitrogen to a fine  
839 powder and stored at -80°C.

840 High molecular weight (HMW) DNA was purified from the powder, essentially as described<sup>1</sup>.  
841 Briefly, nuclei were isolated, digested with proteinase K and lysed with SDS. Here, a standard  
842 watercolor brush with synthetic hair (size 8) was used to re-suspend the nuclei for digestion  
843 and lysis. HMW DNA was purified using phenol-chloroform extraction and precipitation with  
844 ethanol as described<sup>1</sup>. Subsequently, the HMW DNA was dissolved in 50 ml TE (pH 8,0) and  
845 precipitated by the addition of 5 ml 3 M sodium acetate (pH 5,2) and 100 ml ice-cold ethanol.  
846 The suspension was mixed by slow circular movements resulting in the formation of a white  
847 precipitate (HMW DNA), which was collected using a wide-bore 5 ml pipette tip and  
848 transferred for 30 sec into a tube containing 5 ml 75% ethanol. The washing was repeated  
849 twice. The HMW DNA was transferred into a 2 ml tube using a wide-bore tip, collected with a  
850 polystyrene spatula, air-dried in a fresh 2 ml tube and dissolved in 500 µl 10 mM Tris-Cl (pH  
851 8.0). For quantification the Qubit dsDNA High Sensitivity assay kit (Thermo Fisher Scientific,  
852 MA, USA) was used. The DNA size-profile was recorded using the Femto Pulse system and the  
853 Genomic DNA 165 kb kit (Agilent Technologies Inc, CA, USA). In typical experiments the peak  
854 of the size-profile of the HMW DNA for library preparation was around 165 kb.

855

## 856 **DNA library preparation and Pacbio HiFi sequencing**

857

858 For fragmentation of the HMW DNA into 20 kb fragments, a Megaruptor 3 device (speed: 30)  
859 was used (Diagenode, NJ, USA). A minimum of two HiFi SMRTbell libraries were prepared for  
860 each barley genotype following essentially the manufacturer's instructions and the SMRTbell  
861 Express Template Prep Kit (Pacific Biosciences, CA, USA). The final HiFi libraries were size  
862 selected (narrow size range: 18-21 kb) using the SageELF system with a 0,75% Agarose Gel  
863 Cassette (Sage Sciences, MA, USA) according to standard manufacturer's protocols.

864 HiFi CCS reads were generated operating the PacBio Sequel IIe instrument (Pacific Biosciences,  
865 CA, USA) following the manufacturer's instructions. Per genotype about four 8 M SMRT cells  
866 (average yield: 24 Gb HiFi CCS per 8 M SMART cell) were sequenced to obtain an approximate  
867 haploid genome coverage of about 20-fold. In typical experiments the concentration of the  
868 HiFi library on plate was 80-95 pM. 30 h movie time, 2 h pre-extension and sequencing  
869 chemistry v2.0 were used. The resulting raw data was processed using the CCS4 algorithm  
870 (<https://github.com/PacificBiosciences/ccs>).

871

## 872 **Hi-C library preparation and Illumina sequencing**

873

874 *In situ* Hi-C libraries were prepared from one-week old barley seedlings based on the  
875 previously published protocol<sup>2</sup>. Dovetail Omni-C data were generated for Bowman, Aizu6,  
876 Golden Melon, 10TJ18 as per manufacturer's instructions  
877 (<https://dovetailgenomics.com/products/omni-c-product-page/>). Sequencing and Hi-C raw  
878 data processing was performed as described before<sup>3,4</sup>.

879

880

### 881 **Genome sequence assembly and validation**

882 PacBio HiFi reads were assembled using hifiasm (v0.11-r302)<sup>5</sup>. Pseudomolecule construction  
883 was done with the TRITEX pipeline<sup>6</sup>. Chimeric contigs and orientation errors were identified  
884 through manual inspection of Hi-C contact matrices. Genome completeness and consensus  
885 accuracy were evaluated using Merqury (v1.3)<sup>7</sup>. Levels of duplication and heterozygosity were  
886 assessed with Merqury and FindGSE (v1.94)<sup>8</sup>. BUSCO (Benchmarking Universal Single-Copy  
887 Orthologs) (v3.0.2)<sup>9</sup> with the embryophyta\_odb9 data set was run on the final assemblies.

888

### 889 **Single-copy pangenome construction**

890 The single-copy regions in each chromosome-level assembly were identified by filtering 31-  
891 mers occurring more than once in the genomic regions by BBDuk (BBDuk\_37.93,  
892 <https://jgi.doe.gov/data-and-tools/software-tools/bbtools>). Then, the single-copy regions  
893 were obtained in BED format and their sequences were retrieved using BEDTools (v2.29.2)<sup>10</sup>.  
894 The single-copy sequences were clustered using MMseqs2 (Many-against-Many sequence  
895 searching)<sup>11</sup> with the parameters “ --cluster-mode ” and setting over 95% sequence identity.  
896 A representative from each cluster (the largest in a cluster) was selected to estimate the  
897 pangenome size.

898

### 899 **Illumina resequencing**

900 A total of 1,000 plant genetic resources and 315 elite barley varieties (**Supplementary Table**  
901 **5**) were used for whole genome resequencing. Illumina Nextera libraries were prepared and  
902 sequenced on an Illumina NovaSeq 6000 at IPK Gatersleben (**Supplementary Table 5**).

903

### 904 **SNP and SV calling**

905 Reciprocal genome alignment in which each of the pangenome assemblies was aligned to the  
906 MorexV3 assembly with the latter acting either as alignment query or reference. Alignment  
907 was done with Minimap2 (version 2.20)<sup>12</sup>. From the resultant two alignment tables, insertion  
908 and deletions were called by Assemblytics (version 1.2.1)<sup>13</sup> and only deletions were selected  
909 in both alignments to convert into presence/absence variants relative to the Morex reference  
910 genome. Further, balanced rearrangements (inversions, translocations) were scanned for with  
911 SyRI<sup>14</sup>. To call SNPs, raw sequencing reads were trimmed using cutadapt (version 3.3)<sup>15</sup> and  
912 aligned to the MorexV3 reference genome using Minimap2 (version 2.20)<sup>12</sup>. The resulting  
913 alignments were sorted with Novosort (V3.09.01) (<http://www.novocraft.com>). BCFtools  
914 (version 1.9)<sup>16</sup> was used to call SNPs and short insertions and deletions. GWAS for was done  
915 with GEMMA<sup>17</sup>.

916

### 917 **Preparation and Illumina sequencing of narrow-size WGS libraries for core50**

918 10 µg DNA in 130 µl were sheared in tubes (Covaris microTUBE AFA Fiber Pre-Slit Snap Cap)  
919 to an average size of approximately 250 bp using a Covaris S220 focused-ultrasonicator (peak  
920 incidence power: 175 W, duty factor: 10%; cycles per burst: 200; time: 180 sec) according to  
921 standard manufacturer’s protocols (Covaris Ltd., Brighton, UK). The sheared DNA was size  
922 selected using a BluePippin device and a 1.5% agarose cassette with internal R2 marker (Sage  
923 Sciences, MA, USA). A tight size setting at 260 bp was used for the purification of fragments in  
924 the narrow range between 200-300 bp (typical yield: 1-3 µg). The size selected DNA was used  
925 for the preparation of PCR-free whole genome shotgun libraries using the Roche KAPA Hyper  
926 Prep kit according to the manufacturer’s protocols (Roche Diagnostics Deutschland GmbH,

927 Mannheim, Germany). A total of 10 to 12 libraries were provided with unique barcodes,  
928 pooled at equimolar concentrations and quantified by qPCR using the KAPA Library  
929 Quantification Kit for Illumina Platforms according to standard protocols (Roche Diagnostics  
930 Deutschland GmbH, Mannheim, Germany). The pools were sequenced (2x 151 bp, paired-  
931 end) using four S4 XP flowcells and the Illumina NovaSeq 6000 system (Illumina Inc., San  
932 Diego, CA, USA) at IPK Gatersleben.

933

#### 934 **Contig assembly of core50 sequencing data**

935 Raw reads were demultiplexed based on index sequences and duplicate reads were removed  
936 from the sequencing data using Fastuniq<sup>18</sup>. The read1 and read2 sequences were merged  
937 based on the overlap using bbmerge.sh from bbmap (v37.28)<sup>19</sup>. The merged reads were error  
938 corrected using BFC (v181)<sup>20</sup>. The error corrected merged reads were used as an input for  
939 Minia3 (v3.2.0)<sup>21</sup> to assemble reads into unitigs with the following parameters, -no-bulge-  
940 removal -no-tip-removal -no-ec-removal -out-compress 9 -debloom original. The Minia3  
941 source was assembled to enable k-mer size up to 512 as described in the Minia3 manual.  
942 Iterative Minia3 runs with increasing k-mer sizes (100, 150, 200, 250 and 300) were used for  
943 assembly generation as provided in the GATB Minia pipeline ([https://github.com/GATB/gatb-  
944 minia-pipeline](https://github.com/GATB/gatb-minia-pipeline)). In the first iteration, k-mer size of 50 was used to assemble input reads into  
945 unitigs. In the next runs, the input reads as well as the assembly of the previous iteration were  
946 used as input for the minia3 assembler. BUSCO analysis was conducted on the contig  
947 assemblies using BUSCO (v3.0.2) with embryophyta\_odb9 data set<sup>9</sup>. In addition, high-  
948 confidence gene models from Morex V3 reference<sup>22</sup> were aligned to the contig assemblies to  
949 assess completeness with the parameter of  $\geq 90\%$  query coverage and  $\geq 97\%$  identity.

950

#### 951 **Pangenome accession in diversity space**

952 Pseudo-FASTQ paired-end reads (10-fold coverage) were generated from the 76 pangenome  
953 assemblies with fastq\_generator ([https://github.com/johanzi/fastq\\_generator](https://github.com/johanzi/fastq_generator)) and aligned to  
954 MorexV3 reference genome sequence assembly<sup>22</sup> using Minimap2 (version 2.24-r1122, ref.  
955 <sup>12</sup>). SNPs were called together with short-read data (**Supplementary Table 5**) using BCFtools<sup>23</sup>  
956 version 1.9 with the command “mpileup -q 20 -Q20 --excl-flags 3332”. To plot the diversity  
957 space of cultivated barley, the resultant variant matrix was merged with that of 19,778  
958 domesticated barleys of Milner et al.<sup>24</sup> (genotyping-by-sequencing [GBS] data). SNPs with  
959 more than 20 % missing or more than 20 % heterozygous calls were discarded. PCA was done  
960 with smartpca<sup>25</sup> version 7.2.1. To represent the diversity of wild barleys, we used published  
961 GBS and whole-genome sequencing (WGS) data of 412 accessions of that taxon<sup>26,27</sup>. Variant  
962 calling for GBS data was done with BCFtools<sup>23</sup> (version 1.9) using the command “mpileup -q  
963 20 -Q20”. The resultant variant matrix was filtered as follows: (1) only bi-allelic SNP sites were  
964 kept; (2) homozygous genotype calls were retained if their read depth was  $\geq 2$  and  $\leq 50$  and  
965 set to missing otherwise; (3) heterozygous genotype calls were retained if the read depth of  
966 both alleles was  $\geq 2$  and set to missing otherwise. SNPs with more than 20 % missing, more  
967 than 20 % heterozygous calls or a minor allele frequency below 5 % were discarded. PCA was  
968 done with smartpca<sup>25</sup> version 7.2.1. A matrix of pairwise genetic distances based on identity-  
969 by-state (IBS) was computed with Plink2 (version 2.00a3.3LM, ref. <sup>28</sup>) and used to construct an  
970 NJ tree with Fneighbor (<http://emboss.toulouse.inra.fr/cgi-bin/emboss/fneighbor>) in the  
971 EMBOSS package<sup>29</sup>. The tree was visualized with Interactive Tree Of Life (iTOL)<sup>30</sup>.

972

#### 973 **Haplotype representation**



974 Pangenome assemblies were mapped to MorexV3 as described above (“Pangenome accession  
975 in diversity space”). Read depth was calculated with SAMtools<sup>23</sup> version 1.16.1. Genotype calls  
976 were set to missing if they were supported by fewer than two reads. Identity-by-state (IBS)  
977 was calculated with Plink2 (version 2.000a3.3LM, ref. <sup>28</sup>) in 1 Mb windows (shift: 0.5 Mb) using  
978 the using command “--sample-diff counts-only counts-cols=ibs0, ibs1”. Windows which in one  
979 of both accessions in the comparison had 2-fold coverage over less than 200 kb were set to  
980 missing. The number of differences (d) in a window was calculated as  $\text{ibs0} + \text{ibs1} / 2$ , where ibs0  
981 is the number of homozygous differences and ibs1 that of heterozygous ones. This distance  
982 was normalized for coverage by the formula  $d / i \times 1 \text{ Mb}$ , where i is the size in bp of the region  
983 covered in both accessions in the comparison had at least 2-fold coverage. In each window,  
984 we determined for each among the PGR and cultivars panel, the closest pangenome accession  
985 according to the coverage-normalized IBS distance. Only accessions with fewer than 10 %  
986 missing windows due to low coverage were considered, leaving 899 PGRs and 264 cultivars.  
987 The distance to the closest pangenome accession was plotted with the R package ggplot2 to  
988 determine the threshold for similarity (**Extended Data Fig. 2d**).

989

### 990 **Transcriptome sequencing for gene annotation**

991 Data for transcript evidence-based genome annotation was provided by the International  
992 Barley Pan-Transcriptome Consortium, and a detailed description of sample preparation and  
993 sequencing is provided elsewhere. In brief, the 20 genotypes sequenced for the first version  
994 of the barley pangenome<sup>26</sup> were used for transcriptome sequencing. Five separate tissues  
995 were sampled for each genotype. These were: embryo (including mesocotyl and seminal  
996 roots), seedling shoot, seedling root, inflorescence and caryopsis. Three biological replicates  
997 were sampled from each tissue type, amounting to 330 samples. Four samples failed quality  
998 control and were excluded.

999 Preparation of the strand-specific dUTP RNA-Seq libraries, and Illumina paired-end 150 bp  
1000 sequencing were carried out by Novogene (UK) Company Limited. In addition, PacBio Iso-Seq  
1001 sequencing was carried out using a PacBio Sequel IIe sequencer at IPK Gatersleben. For this,  
1002 a single sample per genotype was obtained by pooling equal amounts of RNA from a single  
1003 replicate from all five tissues. Each sample was sequenced on an individual 8M SMRT cell.

1004

### 1005 **De novo gene annotation**

1006 Structural gene annotation was done combining de novo gene calling and homology-based  
1007 approaches with RNAseq, IsoSeq, and protein datasets (**Extended Data Fig. 3a**). Using  
1008 evidence derived from expression data, RNAseq data were first mapped using STAR<sup>31</sup> (version  
1009 2.7.8a) and subsequently assembled into transcripts by StringTie<sup>32</sup> (version 2.1.5, parameters  
1010 -m 150-t -f 0.3). Triticeae protein sequences from available public datasets (UniProt<sup>33</sup>,  
1011 <https://www.uniprot.org>, 05/10/2016) were aligned against the genome sequence using  
1012 GenomeThreader<sup>34</sup> (version 1.7.1; arguments -startcodon -finalstopcodon -species rice -  
1013 gcmincoverage 70 -prseedlength 7 -prhdist 4). Isoseq datasets were aligned to the genome  
1014 assembly using GMAP<sup>35</sup> (version 2018-07-04). All assembled transcripts from RNAseq, IsoSeq,  
1015 and aligned protein sequences were combined using Cuffcompare<sup>36</sup> (version 2.2.1) and  
1016 subsequently merged with StringTie (version 2.1.5, parameters --merge -m150) into a pool of  
1017 candidate transcripts. TransDecoder (version 5.5.0; <http://transdecoder.github.io>) was used  
1018 to identify potential open reading frames and to predict protein sequences within the  
1019 candidate transcript set.

1020 *Ab initio* annotation was initially done using Augustus<sup>37</sup> (version 3.3.3). GeneMark<sup>38</sup> (version  
1021 4.35) was additionally employed to further improve structural gene annotation. To avoid  
1022 potential over-prediction, we generated guiding hints using the above described RNAseq,  
1023 protein, and IsoSeq datasets as described before<sup>39</sup>. A specific Augustus model for barley was  
1024 built by generating a set of gene models with full support from RNAseq and IsoSeq. Augustus  
1025 was trained and optimized following a published protocol<sup>39</sup>. All structural gene annotations  
1026 were joined using EVIDENCEModeller<sup>40</sup> (version 1.1.1), and weights were adjusted according  
1027 to the input source: *ab initio* (Augustus: 5, GeneMark: 2), homology-based (10). Additionally,  
1028 two rounds of PASA<sup>41</sup> (version 2.4.1) were run to identify untranslated regions and isoforms  
1029 using the above described IsoSeq datasets.

1030 We used BLASTP<sup>42</sup> (ncbi-blast-2.3.0+, parameters -max\_target\_seqs 1 -evalue 1e-05) to  
1031 compare potential protein sequences with a trusted set of reference proteins (Uniprot  
1032 Magnoliophyta, reviewed/Swissprot, downloaded on 3 Aug 2016; <https://www.uniprot.org>).  
1033 This differentiated candidates into complete and valid genes, non-coding transcripts,  
1034 pseudogenes, and transposable elements. In addition, we used PTREP (Release 19;  
1035 <http://botserv2.uzh.ch/kelldata/trep-db/index.html>), a database of hypothetical proteins  
1036 containing deduced amino acid sequences in which internal frameshifts have been removed  
1037 in many cases. This step is particularly useful for the identification of divergent transposable  
1038 elements with no significant similarity at the DNA level. Best hits were selected for each  
1039 predicted protein from each of the three databases. Only hits with an e-value below 10e-10  
1040 were considered. Furthermore, functional annotation of all predicted protein sequences was  
1041 done using the AHRD pipeline (<https://github.com/groupschoof/AHRD>).

1042 Proteins were further classified into two confidence classes: high and low. Hits with subject  
1043 coverage (for protein references) or query coverage (transposon database) above 80% were  
1044 considered significant and protein sequences were classified as high-confidence using the  
1045 following criteria: protein sequence was complete and had a subject and query coverage  
1046 above the threshold in the UniMag database or no BLAST hit in UniMag but in UniPoa and not  
1047 PTREP; a low-confidence protein sequence was incomplete and had a hit in the UniMag or  
1048 UniPoa database but not in PTREP. Alternatively, it had no hit in UniMag, UniPoa, or PTREP,  
1049 but the protein sequence was complete. In a second refinement step, low-confidence proteins  
1050 with an AHRD-score of 3\* were promoted to high-confidence.

1051

### 1052 **Transposon masking for de novo gene detection**

1053 The 20 barley accessions with expression data were softmasked for transposons prior to the  
1054 *de novo* gene detection using the REdat\_9.7\_Triticeae section of the PGSB transposon  
1055 library<sup>43</sup>. Vmatch (<http://www.vmatch.de>) was used as matching tool with the following  
1056 parameters: identity>=70%, minimal hit length 75 bp, seedlength 12 bp (vmmatch -d -p -l 75  
1057 -identity 70 -seedlength 12 -exdrop 5 -qmaskmatch tolower). The percentage masked was  
1058 around 80% and almost identical for all 20 accessions.

1059

### 1060 **Gene projections**

1061 Gene contents of the remaining 56 barley genotypes were modelled by the projection of high  
1062 confidence (HC) genes based on evidence-based gene annotations of the 20 barley genotypes  
1063 described above. The approach was similar to and built upon a previously described method<sup>26</sup>.  
1064 To reduce computational load, 760,078 HC-genes of the 20 barley annotations were clustered  
1065 by cd-hit<sup>44</sup> requiring 100% protein sequence similarity and a maximal size difference of four  
1066 amino acids. The resulting 223,182 source genes were subsequently used for all downstream

1067 projections as non-redundant transcript set representative for the evidence-based  
1068 annotations. For each source, its maximal attainable score was determined by global protein  
1069 self-alignment using the Needleman-Wunsch algorithm as implemented in Biopython<sup>45</sup> v1.8  
1070 and the blosum62 substitution matrix<sup>46</sup> with a gap open and extension penalty of 0.5 and  
1071 10.0, respectively.

1072 Next, we surveyed each barley genome sequence using minimap2 (ref. <sup>12</sup>) with options ‘-ax  
1073 splice:hq’ and ‘-uf’ for genomic matches of source transcripts. Each match was scored by its  
1074 pairwise protein alignment with the source sequence that triggered the match. Only complete  
1075 matches with start and stop codons and a score  $\geq 0.9$  of the source self-score (see above) were  
1076 retained. The source models were classified into four bins by decreasing confidence qualities:  
1077 with or without pfam domains, plastid- and transposon-related genes. Projections were  
1078 performed stepwise for the four qualities, starting from the highest to the lowest. In each  
1079 quality group, matches were then added into the projected annotation if they did not overlap  
1080 with any previously inserted model by their coding region. Insertion order progressed from  
1081 the top to the lowest scoring match. In addition, we tracked the number of insertions for each  
1082 source by its identifier. For the two top quality categories, we performed two rounds of  
1083 projections, firstly inserting each source maximally only once followed by rounds allowing one  
1084 source inserted multiple times into the projected annotation. To consolidate the 20 evidence-  
1085 based, initial annotations for any genes potentially missed, we employed an identical  
1086 approach but inserted any non-overlapping matches starting from the prior RNA-seq based  
1087 annotation. Phylogenetic Hierarchical Orthogroups (HOGs) based on the primary protein  
1088 sequences from 76 annotated barley genotypes were calculated using Orthofinder<sup>47</sup> version  
1089 2.5.5 (standard parameters). Conserved HOGs contain at least one gene model from all 76  
1090 barley genotypes. Variable HOGs contain gene models from at least one barley genotypes and  
1091 at most 75 barley genotypes. The distribution of all HOG configurations is provided in  
1092 **Extended Data Fig. 3b**. GENESPACE<sup>48</sup> was used to determine syntenic relationships between  
1093 the chromosomes of all 76 genotypes.

1094

### 1095 **Whole-genome pangenome graphs**

1096 Genome graphs were constructed using Minigraph<sup>49</sup> version 0.20-r559. Other graph  
1097 construction tools (PGGB<sup>50</sup>, Minigraph-Cactus<sup>51</sup>) turned out to be computationally prohibitive  
1098 for a genome of this size and complexity, combined with the large number of accessions used  
1099 in this investigation. Minigraph does not support small variants (< 50 bp), thus graph  
1100 complexity is lower than with other tools. However, even with Minigraph, graph construction  
1101 at the whole genome level was computationally prohibitive and thus graphs had to be  
1102 computed separately for each chromosome, precluding detection of interchromosomal  
1103 translocations.

1104 Graph construction was initiated using the Morex V3 assembly<sup>52</sup> as a reference. The remaining  
1105 assemblies were added into the graph sequentially, in order of descending dissimilarity to  
1106 Morex. Structural variants were called after each iteration using gfatools bubble (v. 0.5-r250-  
1107 dirty, <https://github.com/lh3/gfatools>). Following graph construction, the input sequences of  
1108 all accessions were mapped back to the graph using Minigraph with the “--call” option  
1109 enabled, which generates a path through the graph for each accession. The resulting BED  
1110 format files were merged using Minigraph’s mgutils.js utility script to convert them to P lines  
1111 and then combined with the primary output of Minigraph in the proprietary RGFA format  
1112 (<https://github.com/lh3/gfatools/blob/master/doc/rGFA.md>). Graphs were then converted  
1113 from RGFA format to GFA format (<https://github.com/GFA-spec/GFA->

1114 spec/blob/master/GFA1.md) using the “convert” command from the vg toolkit<sup>53</sup> version  
1115 v1.46.0 "Altamura". This step ensures that graphs are compatible with the wider universe of  
1116 graph processing tools, most of which require GFA format as input. Chromosome-level graphs  
1117 were then joined into a whole-genome graph using vg combine. The combined graph was  
1118 indexed using vg index and vg gbwt, two components of the the vg toolkit<sup>53</sup>.

1119 General statistics for the whole-genome graph were computed with vg stats. Graph growth  
1120 was computed using the heaps command from the ODGI toolkit<sup>54</sup> version 0.8.2-0-g8715c55,  
1121 followed by plotting with its companion script heaps\_fit.R. The latter also computes values for  
1122 gamma, the slope coefficient of Heap’s law which allows the classification of pangenome  
1123 graphs into open or closed pangenomes, i.e. a prediction of whether the addition of further  
1124 accessions would increase the size of the pangenome<sup>55</sup>.

1125 Structural variant (SV) statistics were computed based on the final BED file produced after the  
1126 addition of the last line to the graph. A custom shell script was used to classify variants  
1127 according to the Minigraph custom output format. This allows the extraction of simple, i.e.  
1128 non-nested, insertions and deletions (relative to the MorexV3 graph backbone), as well simple  
1129 inversions. The remaining SVs fall into the “complex” category where there can be multiple  
1130 levels of nesting of different variant types and this precluded further, more fine-grained  
1131 classification.

1132 To elucidate the effect of a graph-based reference on short read mapping, we obtained whole  
1133 genome shotgun Illumina reads from five barley samples (**Extended Data Fig. 4b**) in the  
1134 European Nucleotide Archive (ENA) and mapped these onto the whole genome graph using  
1135 vg giraffe<sup>56</sup>. For comparison with the standard approach of mapping reads to a linear single  
1136 genome reference, we mapped the same reads to the Morex V3 reference genome sequence  
1137 assembly<sup>52</sup> with bwa mem<sup>57</sup> version 0.7.17-r1188. Mapping statistics were computed with  
1138 vg<sup>53</sup> stats and samtools<sup>23</sup> stats (version 1.9), respectively.

1139

### 1140 **Analysis of the *Mla* locus**

1141

1142 The coordinates and sequences of the 32 genes present at the *Mla* locus were extracted from  
1143 the MorexV3 genome sequence assembly<sup>52</sup>. To find the corresponding position and copy  
1144 number in each of the 76 genomes, we used BLAST<sup>42</sup> (-perc\_identity: 90, -word\_size:11, all  
1145 other parameters set as default). The expected BLAST result for a perfectly conserved allele is  
1146 a long fragment (exon\_1) of 2,015 bp follow by a gap of ~1,000 bp due to the intron and  
1147 another fragment (exon\_2) of 820 bp. To detect the number of copies, first multiple BLAST  
1148 results for a single gene were merged if two different BLAST segments were within 1.1kb. Then  
1149 only if the total length of the input was found, this was counted as a copy. To analyse the  
1150 structural variation across all 76 accessions, the non-filtered BLAST results were plotted in a  
1151 region of -20,000 and +500,000 base pairs around the start of the BPM gene  
1152 HORVU.MOREX.r3.1HG0004540 that was used as an anchor (present in all 76 lines,  
1153 Supplementary Figure 1. To detection the different *Mla* alleles, three different threshold of -  
1154 Perc\_identity for the BLAST were used: 100, 99 and 98.

1155

### 1156 **Scan for structurally complex loci**

1157 We utilised a pipeline developed by Rabanus-Wallace et al. <sup>58</sup> that performs sequence-  
1158 agnostic identification of long-duplication-prone-regions (L-DPRs) in a reference genome,  
1159 followed by identification of gene families with a statistical tendency to occur within L-DPRs.  
1160 The pipeline assumes that a candidate L-DPR will contain an elevated concentration of locally

1161 repeated sequences in the kb-scale length range. We first aligned the MorexV3 genome  
1162 sequence assembly<sup>52</sup> against itself using lastz<sup>59</sup> (v1.04.03; arguments: '--notransition --  
1163 step=500 -gapped'). For practicality purposes, this was done in 2 Mb blocks with a 200 kb  
1164 overlap, and any overlapping I-DPRs identified in multiple windows were merged. For each  
1165 window, we ignored the trivial end-to-end alignment, and of the remaining alignments,  
1166 retained only those longer than 5 kb and falling fully within 200 kb of one and another. An  
1167 alignment 'density' was calculated over the chromosome by calculating, at 'interrogation  
1168 points' spaced equally at 1 kb intervals along the length of the chromosome, an alignment  
1169 density score that is simply the sum of all the lengths of any of the filtered alignments  
1170 spanning that interrogation point. A Gaussian kernel density (bandwidth 10 kbp) was  
1171 calculated over these the interrogation points, weighted by their scores. To allow  
1172 comparability between windows, the interrogation point densities were normalised by the  
1173 sum of scores in the window. Runs of interrogation points at which the density surpassed a  
1174 minimum density threshold were flagged as I-DPRs. A few minor adjustments to these regions  
1175 (merging of overlapping regions, and trimming<sup>59</sup> the end coordinates to ensure the stretches  
1176 always begin and end in repeated sequence) yielded the final tabulated list of I-DPR  
1177 coordinates (**Supplementary Table 7**). The method was implemented in R making use of the  
1178 package data.table. Genes in each I-DPRs were clustered with UCLUST<sup>60</sup> (v11, default  
1179 parameters) using a protein clustering distance cutoff of 0.5 and for each cluster the most  
1180 frequent functional description as per the MorexV3 gene annotation<sup>52</sup> was assigned as the  
1181 functional description of the cluster.

1182

### 1183 **Molecular dating of divergence times of duplicated genes in complex loci**

1184 For molecular dating of gene duplications, we used segments of up to 4 kb, starting 1 kb  
1185 upstream of duplicated genes in complex loci. With this, we presumed to only use intergenic  
1186 sequences which are free from selection pressure and thus evolve at a neutral rate of  $1.3 \times 10^{-8}$   
1187 substitutions per site per year<sup>61</sup>. The upstream sequences of all duplicated genes of  
1188 respective complex locus were then aligned pairwise with the program Water from the  
1189 EMBOSS package<sup>29</sup> (obtained from Ubuntu repositories, ubuntu.com). This was done for all  
1190 gene copies of all barley accession for which multiple gene copies were found. Molecular  
1191 dating of the pairwise alignments was done as previously described<sup>62</sup> using the substitution  
1192 rate of  $1.3 \times 10^{-8}$  substitutions per site per year<sup>61</sup>.

1193

### 1194 ***Amy1\_1* analysis in pangenome assemblies**

1195 The *amy1\_1* gene copy HORVU.MOREX.PROJ.6HG00545380 was used was used to BLAST  
1196 against all 76 genome assemblies. Full-length sequences with identity over 95% were  
1197 extracted and used for further analyses. Unique sequences were identified by clustering at  
1198 100% identity using CD-Hit<sup>44</sup> and were aligned using MAFFT<sup>63</sup> v7.490. Sequence variants  
1199 among *amy1\_1* gene copies at genomic DNA, CDS and respective protein level were collected  
1200 and *amy1\_1* haplotypes (i.e. the combinations of copies) in each genotype assembly were  
1201 summarized using R<sup>64</sup> v4.2.2. A Barke-specific SNP locus  
1202 (GGCGCCAGGCATGATCGGGTGGTGGCCAGCCAAGGCGGTGACCTTCGTGGACAACCACGACACCG  
1203 GCTCCACGCAGCACATGTGGCCCTCCCTTCTGACA[A/G]GGTCATGCAGGGATATGCGTACATACTCA  
1204 CGCACCCAGGGACGCCATGCATCGTGAGTTCGTGTCGTACCAATACATCACATCTCAATTTCTTTCTTGT  
1205 TTCGTTTCATAA) for *amy1\_1* haplotype cluster ProtHap3 (**Supplementary Table 20**) was  
1206 identified and used for KASP marker development (LGC Biosearch Technologies, Hoddesdon,  
1207 United Kingdom).



1208

### 1209 **Comparative analysis of the *amy1\_1* locus structure**

1210 Based on the genome annotation of cv. Morex, 15 gene sequences on either side of *amy1\_1*  
1211 gene copy HORVU.MOREX.PROJ.6HG00545440 were extracted. The 31 genes were compared  
1212 against the 76 genome assemblies using NCBI-BLAST<sup>42</sup> (BLASTN, word\_size of 11 and percent  
1213 identity of 90, other parameters as default). Alignment plots were generated from the BLAST  
1214 result coordinates by scaling based on the mid-point between  
1215 HORVU.MOREX.r3.6HG0617300/HORVU.MOREX.PROJ.6HG00545250 and  
1216 HORVU.MOREX.r3.6HG0617710/HORVU.MOREX.PROJ.6HG00545670. All BLAST results in the  
1217 region (+/- 1Mb) around this mid-point were plotted using R<sup>64</sup>.

1218

### 1219 ***Amy1\_1* PacBio amplicon sequencing.**

1220 Genomic DNA from one-week old Morex seedling leaves was extracted with DNeasy<sup>®</sup> Plant  
1221 Mini Kit (QIAGEN GmbH, Hilden, Germany). Based on the MorexV3 genome sequence  
1222 assembly<sup>52</sup>, *amy1\_1* full-length copy-specific primers were designed using Primer3 (ref. <sup>65</sup>)  
1223 (<https://primer3.ut.ee/>): 6F - GTAGCAGTGCAGCGTGAAGTC, 80F -  
1224 AGACATCGTTAACCACACATGC, 82F - GTTCTCGTCCCTTGCCTTAA, 82F -  
1225 GTTCTCGTCCCTTGCCTTAA, 33R - GATCTGGATCGAAGGAGGGC, 79R -  
1226 TCATACATGGGACCAGATCGAG, 80R - ACGTCAAGTTAGTAGGTAGCCC. All forward primers were  
1227 tagged with bridge sequence (preceding T to primer name)  
1228 [AmC6]gcagtcgaacatgtagctgactcaggtcac, while reverse primers were tagged with  
1229 [AmC6]tggatcactgtgcaagcatcacatcgtag to allow annealing to barcoding primers. These bridge  
1230 sequence-tagged gene-specific primers were used in pairs with each other targeting 1-2  
1231 copies of 3-6 kb *amy1\_1* genes, including upstream and downstream 500-1000 bp regions:  
1232 T6F + T33R, T6F + T79R, T80F + T80R and T82F + T80R. A two-step PCR protocol was  
1233 conducted. The first step PCR reaction was prepared in 25 µl volume using 2 µl DMSO, 0.3 µl  
1234 Q5 polymerase (New England Biolab, Massachusetts, United States), 1 µl *amy1\_1*-specific  
1235 primer pair (10 µM each), 2 µl gDNA, 0.5 µl dNTPs (10mM), 5 µl Q5 buffer and H<sub>2</sub>O. The PCR  
1236 program was as following: initial denaturation at 98°C/1min followed by 25-28 cycles of  
1237 98°C/30 sec, 58°C/30 sec, and 72°C/3 min for extension, with a final extension step of 72°C/2  
1238 min. The second PCR step (barcoding PCR) was prepared in the same way using 1 µl of the first  
1239 PCR product as DNA template, barcoding primers (Pacific Biosciences of California, Inc.,  
1240 California, United States) and the PCR program reduced to 20 cycles. After quality check on  
1241 1% agarose gel, all barcoded PCR products were mixed and purified with AMPure<sup>®</sup> PB (Pacific  
1242 Biosciences of California, Inc., California, United States). The SMRT bell library preparation and  
1243 sequencing were carried out at BGI Tech Solutions (BGI Tech Solutions Co., Ltd., Hongkong,  
1244 China). Sequencing data was analysed using SMRT Link v.10.2. To minimize PCR chimeric noise,  
1245 CCS were first constructed for each molecule. Secondly, Long Amplicon Analysis (LAA) was  
1246 carried out based on subreads from 50 bp window spanning peak positions of all CCS length.  
1247 Final consensus sequences for each *amy1\_1* was determined with the aid of size estimation  
1248 from agarose gel imaging.

1249

### 1250 ***Amy1\_1* SNP haplotype analysis and k-mer based copy number estimation.**

1251 SNP haplotypes were analyzed in 1,315 plant genetic resources and elite varieties in the  
1252 extended *amy1\_1*-cluster region (MorexV3 chr6H: 516,385,490 - 517,116,415 bp). SNPs with  
1253 >20% missing data among the analyzed lines and minor allele frequency (MAF) < 0.01 were  
1254 removed from downstream analyses. The data was converted to 0,1 and 2 format using

1255 VCFtools<sup>66</sup> and samples were clustered using pheatmap package ([https://cran.r-](https://cran.r-project.org/web/packages/pheatmap/pheatmap.pdf)  
1256 [project.org/web/packages/pheatmap/pheatmap.pdf](https://cran.r-project.org/web/packages/pheatmap/pheatmap.pdf)) from R statistical environment<sup>58</sup>. The  
1257 sequential clustering approach was used to achieve the desired separation. At each step, two  
1258 extreme clusters were selected and then samples from each cluster were clustered separately.  
1259 The process was repeated until the desired separation was achieved based on visual  
1260 inspection.

1261 K-mers (k=21) were generated from Morex *amy1\_1* gene family member's conserved region  
1262 using jellyfish<sup>67</sup> v2.2.10. After removing k-mers with counts from regions other than *amy1\_1*  
1263 in the Morex V3 genome assembly, k-mers were counted in the Illumina raw reads  
1264 (**Supplementary Table 5**) using Seal (BBtools, [https://jgi.doe.gov/data-and-tools/software-](https://jgi.doe.gov/data-and-tools/software-tools/bbtools/)  
1265 [tools/bbtools/](https://jgi.doe.gov/data-and-tools/software-tools/bbtools/)). All k-mer counts were normalized to counts per MorexV3 genome and  
1266 *amy1\_1* copy number was estimated as the median count of all k-mers from each accession  
1267 in R.

1268 Estimation ability was validated by comparing copy number from pangenome assemblies and  
1269 short-read sequencing data (**Extended Data Fig. 8c**). For 1,000 plant genetic resources,  
1270 countries ( $\geq 10$  accessions) were color shaded based on their proportions of accessions with  
1271 *amy1\_1* copy number  $> 5$  on a world map using the R package maptools ([https://cran.r-](https://cran.r-project.org/web/packages/maptools/index.html)  
1272 [project.org/web/packages/maptools/index.html](https://cran.r-project.org/web/packages/maptools/index.html)).

1273

#### 1274 **AMY1\_1 protein structure and protein folding simulation**

1275 The published protein structure of  $\alpha$ -amylase AMY1\_1 from accession Menuet, in complex  
1276 with the pseudo-tetrasaccharide acarbose (PDB:1bg9; ref. <sup>68</sup>), was used to simulate the  
1277 structural context of the amino acid variants identified in barley accessions Morex, Barke and  
1278 RGT Planet. The amino acid sequence of the crystalized AMY1\_1 protein from Menuet and  
1279 the Morex reference copy *amy1\_1* HORVU.MOREX.PROJ.6HG00545380 used in this study are  
1280 identical. The protein was visualized using PyMol 2.5.5 (Schrödinger Inc. New York, NY, USA).  
1281 The Dynamut2 webserver<sup>69</sup> was used to predict changes in protein stability and dynamics by  
1282 introducing amino acid variants identified in the Morex, Barke and RGT Planet genome  
1283 assemblies.

1284

#### 1285 **Development of diverse *amy1\_1* haplotype barley near-isogenic lines**

1286 Near-isogenic lines (NILs) with different *amy1\_1* haplotypes were derived from crosses  
1287 between RGT Planet as recipient and Barke or Morex *amy1\_1*-cluster donor parents  
1288 (ProtHap3, ProtHap4 and ProtHap0, respectively; **Supplementary Table 20**), followed by two  
1289 subsequent backcrosses to RGT Planet and one selfing step (BC<sub>2</sub>S<sub>1</sub>) to retrieve homozygous  
1290 plants at the *amy1\_1* locus. A total of four *amy1\_1*-Barke NILs (ProtHap3) and one *amy1\_1*-  
1291 Morex NIL (ProtHap0) were developed and tested against RGT Planet (ProtHap4) replicates.  
1292 Plants were grown in a greenhouse at 18°C under 16/8-hour light/dark cycles. Foreground and  
1293 background molecular markers were used in each generation to assist plant selection.  
1294 Respective BC<sub>2</sub>S<sub>1</sub> plants were genotyped with the Barley Illumina 15K array (SGS Institut  
1295 Fresenius GmbH, TraitGenetics Section, Germany) and grown to maturity. Grains were  
1296 harvested and further propagated in field plots in consecutive years in various locations (Nørre  
1297 Aaby, Denmark; Lincoln, New Zealand; Maule, France). Grains from field plots were harvested  
1298 and threshed using a Wintersteiger Elite plot combiner (Wintersteiger AG, Germany), and  
1299 sorted by size (threshold, 2.5 mm) using a Pfeuffer SLN3 sample cleaner (Pfeuffer GmbH,  
1300 Germany).

1301

### 1302 **Micro-malting and $\alpha$ -amylase activity analysis**

1303 Non-dormant barley samples of RGT Planet and respective NILs with different *amy1\_1*  
1304 haplotypes (50g each, graded >2.5 mm) were micro-malted in perforated stainless-steel  
1305 boxes. The barley samples were steeped at 15 °C by submersion of the boxes in water.  
1306 Steeping took place for six hours on day one, three hours on day two and one hour on day  
1307 three, followed by air rests, to reach 35%, 40% and 45% water content, respectively. The actual  
1308 water uptake of individual samples was determined as the weight difference between initial  
1309 water content, measured with Foss 1241 NIT instrument (Foss A/S, Hillerød, Denmark), and  
1310 the sample weight after surface water removal. During air rest, metal beakers were placed  
1311 into a germination box at 15°C. Following the last steep, the barley samples were germinated  
1312 for 3 days at 15°C. Finally, barley samples were kiln dried in an MMK Curio kiln (Curio Group  
1313 Ltd, Buckingham, England) using a two-step ramping profile. First ramping step started at a set  
1314 point of 27°C and a linear ramping at 2°C/h to the breakpoint at 55°C using 100% fresh air.  
1315 Second linear ramping was at 4°C/h reaching a maximum at 85°C. This temperature was kept  
1316 constant for 90 minutes using 50% air recirculation. The kilned samples were then deculmed  
1317 using a manual root removal system (Wissenschaftliche Station für Brauerei, Munich,  
1318 Germany).  $\alpha$ -amylase activity was measured using the Ceralpha method (Ceralpha Method  
1319 MR-CAAR4, Megazyme) modified for Gallery Plus Beermaster (Thermo Fisher Scientific, USA).

1320

### 1321 **Rachilla hair ploidy measurements**

1322 Ploidy assessment was performed on rachillae harvested from barley spikes at developmental  
1323 stage<sup>70</sup> ~W9.0. Once isolated, rachillae were fixed with 50% Ethanol/10% acetic acid for 16h  
1324 after which they were stained with 1  $\mu$ M 4',6-Diamidino-2-phenylindol (DAPI) in 50 mM  
1325 phosphate buffer (pH 7.2) supplemented with 0.05% Triton X100. Probes were analyzed with  
1326 a Zeiss LSM780 confocal laser scanning microscope using a 20x NA 0.8 objective, zoom 4x, and  
1327 image size 512 x 512 pixel. DAPI was visualized with a 405 nm laser line in combination with a  
1328 405–475 nm bandpass filter. Pinhole was set to ensure the whole nucleus was measured in  
1329 one scan. Size and fluorescence intensity of the nuclei were measured with ZEN black (ZEISS)  
1330 software. For data normalization small round nuclei of the epidermal proper were used for 2C  
1331 calibration.

1332

### 1333 **Scanning electron microscopy**

1334 Sample preparation and recording by scanning electron microscopy was essentially performed  
1335 as described previously<sup>71</sup>. In brief, samples were fixed overnight at 4°C in 50 mM phosphate  
1336 buffer (pH 7.2) containing 2% v/v glutaraldehyde and 2% v/v formaldehyde. After washing  
1337 with distilled water and dehydration in an ascending ethanol series, samples were critical  
1338 point-dried in a Bal-Tec critical point dryer (Leica microsystems, [https://www.leica-](https://www.leica-microsystems.com)  
1339 [microsystems.com](https://www.leica-microsystems.com)). Dried specimens were attached to carbon-coated aluminium sample  
1340 blocks and gold-coated in an Edwards S150B sputter coater (Edwards High Vacuum Inc.,  
1341 <http://www.edwardsvacuum.com>). Probes were examined in a Zeiss Gemini30 scanning  
1342 electron microscope (Carl Zeiss Microscopy GmbH, <https://www.zeiss.de>) at 5 kV acceleration  
1343 voltage. Images were digitally recorded.

1344

### 1345 **Linkage mapping of *SHORT RACHILLA HAIR 1 (HvSRH1)***

1346 Initial linkage mapping was performed using genotyping-by-sequencing (GBS) data of a large  
1347 'Morex' x 'Barke' F<sub>8</sub> RIL population<sup>72</sup> (ENA project PRJEB14130). The GBS data of 163 RILs,  
1348 phenotyped for rachilla hair in the F<sub>11</sub> generation, and the two parental genotypes were

1349 extracted from the variant matrix using VCFtools<sup>66</sup> and filtered as described previously<sup>24</sup> for a  
1350 minimum depth of sequencing to accept heterozygous and homozygous calls of 4 and 6,  
1351 respectively, a minimum mapping quality score of the SNPs of 30, a minimal fraction of  
1352 homozygous calls of 30 %, and a maximum fraction of missing data of 25%. The linkage map  
1353 was built with the R package ASMap<sup>73</sup> using the MSTMap algorithm<sup>74</sup> and the Kosambi  
1354 mapping function, forcing the linkage group to split according to the physical chromosomes.  
1355 The linkage mapping was done with R/qtl<sup>75</sup> using the binary model of the scanone function  
1356 with the EM method<sup>76</sup>. The significance threshold was calculated running 1000 permutations  
1357 and the interval was determined by a LOD drop of 1. To confirm consistency between the F<sub>8</sub>  
1358 RIL genotypes and F<sub>11</sub> RIL phenotypes, three PCR Allele Competitive Extension (PACE) markers  
1359 were designed through 3CR Bioscience (Essex, UK) free assay design service, using  
1360 polymorphisms between the genome assemblies of the two parents (**Supplementary Table**  
1361 **23**), and PACE genotyping was performed as described earlier<sup>77</sup>. To reduce the *Srh1* interval,  
1362 22 recombinant F<sub>8</sub> RILs were sequenced by Illumina whole-genome sequencing (WGS), the  
1363 sequencing reads were mapped on MorexV3 reference genome<sup>52</sup>, and the SNP called. The 100  
1364 bp region around the flanking SNPs of the *Srh1* interval as well as the sequence of the  
1365 candidate gene HORVU.MOREX.r3.5HG0492730 were compared to the pangenome  
1366 assemblies using BLASTN<sup>78</sup> to identify the corresponding coordinates and extract the  
1367 respective intervals for comparison. Gene sequences were aligned with Muscle5 (ref. <sup>79</sup>).  
1368 Structural variation between intervals was assessed with LASTZ<sup>59</sup> version 1.04.03. The motif  
1369 search was carried out with the EMBOSS<sup>80</sup> 6.5.7 tool fuzznuc.  
1370

### 1371 **Cas9-mediated mutagenesis**

1372 Guide RNA (gRNA) target motifs in the 'Golden Promise' *HvSrh1* candidate gene  
1373 HORVU.GOLDEN\_PROMISE.PROJ.5HG00440000.1 were selected by using the online tool WU-  
1374 CRISPR<sup>81</sup> to induce translational frameshift mutations by insertion/deletion of nucleotides  
1375 leading to loss-of-function of the gene. One pair of target motifs (gRNA1a:  
1376 CCTCGCTGCCCGCCGACGC, gRNA1b: GACAAGACGAAGGCCGCGG) was selected within the  
1377 *HvSrh1* candidate gene based on their position within the first half of the coding sequence  
1378 and the two-dimensional minimum free energy structures of the cognate single-gRNAs  
1379 (NNNNNNNNNNNNNNNNNNNGUUUUAGAGCUAGAAAUAAGCAAGUUAAAAUAAGGCUAGUC  
1380 CGUUAUCAACUUGAAAAAGUGGCACCGAGUCGGUGCUUUU) as modelled by the RNAfold  
1381 WebServer<sup>82</sup> and validated as suggested by Koeppel et al. <sup>83</sup>. gRNA-containing transformation  
1382 vectors were cloned using the modular CasCADE vector system  
1383 (<https://doi.org/10.15488/13200>). gRNA-specific sequences were ordered as DNA  
1384 oligonucleotides (**Supplementary Table 24**) with specific overhangs for BsaI-based cloning  
1385 into the gRNA-module vectors carrying the gRNA scaffold, driven by the *Triticum aestivum* U6  
1386 promoter. Golden Gate assembly of gRNAs and the *cas9* module, driven by the *Zea mays*  
1387 *Polyubiquitin 1 (ZmUbi1)* promoter, were performed according to the CasCADE protocol to  
1388 generate the intermediate vector pHP21. To generate the binary vector pHP22, the gRNA and  
1389 *cas9* expression units were cloned using SfiI into the generic vector<sup>84</sup> p6i-2x35S-TE9 that  
1390 harbours an *hpt* gene under control of a doubled-enhanced *CaMV35S* promoter in its transfer-  
1391 DNA for plant selection. *Agrobacterium*-mediated DNA transfer to immature embryos of the  
1392 spring barley Golden Promise was performed as previously described<sup>85</sup>. In brief, immature  
1393 embryos were excised from caryopses 12-14 days after pollination and co-cultivated with  
1394 *Agrobacterium* strain AGL1 carrying pHP22 for 48 hours. Then, the explants were cultivated  
1395 for further callus formation under selective conditions using Timentin and hygromycin, which



1396 was followed by plant regeneration. The presence of T-DNA in regenerated plantlets was  
1397 confirmed by *hpt*- and *cas9*-specific PCRs (primer sequences in **Supplementary Table 24**).  
1398 Primary mutant plants ( $M_1$  generation) were identified by PCR amplification of the target  
1399 region (primer sequences in **Supplementary Table 24**) followed by Sanger sequencing at LGC  
1400 Genomics GmbH (Berlin, Germany). Double or multiple peaks in the sequence chromatogram  
1401 starting around the Cas9 cleavage site upstream of the target's protospacer-adjacent motif  
1402 (PAM) were considered as an indication for chimeric and/or heterozygous mutants. Mutant  
1403 plants were grown in a glasshouse until the formation of mature grains.  $M_2$  plants were grown  
1404 in a climate chamber under speed breeding conditions (22 h light at 22 °C and 2 h dark at 19  
1405 °C, adapted from Watson et al.<sup>86</sup> and genotyped by Sanger sequencing of PCR amplicons as  
1406 given above.  $M_2$  grains were subjected to phenotyping.

1407

#### 1408 **FIND-IT library construction**

1409 We constructed a FIND-IT library in cv. 'Etincel' (6-row winter malting barley; SECOBRA  
1410 Recherches) as described in Knudsen et al.<sup>87</sup>. In short, we induced mutations by incubating  
1411 2.5 kg of 'Etincel' grain in water overnight at 8°C following an incubation in 0.3 mM NaN<sub>3</sub> at  
1412 pH 3.0 for 2 hours at 20°C with continuous application of oxygen. After thoroughly washing  
1413 with water, the grains were air-dried in a fume hood for 48 hours. Mutagenized grains were  
1414 sown in fields in Nørre Aaby, Denmark, and harvested in bulk using a Wintersteiger Elite plot  
1415 combiner (Wintersteiger AG, Germany). In the following generation, 2.5 kg of grain was sown  
1416 in fields in Lincoln, New Zealand, and 188 pools of approximately 300 plants each were hand-  
1417 harvested and threshed. A representative sample, 25% of each pool, was milled (Retsch  
1418 GM200, Haan, Germany), and DNA was extracted from 25 g of the flour by LGC Genomics  
1419 GmbH (Berlin, Germany).

1420

#### 1421 **FIND-IT screening**

1422 The FIND-IT 'Etincel' library was screened as described in Knudsen et al.<sup>87</sup> using a single assay  
1423 for the isolation of *srh1*<sup>P635</sup> variant [ID# CB-FINDit-Hv-014]. Forward primer 5'  
1424 AATCCTGCAGTCCTTGG 3', reverse primer 5' GAGGAGAAGAAGGAGCC 3', mutant probe 5'-6-  
1425 FAM/CGTGGACGT/ZEN/CGACG/3'IABkFQ/ Wild type probe  
1426 /5'SUN/ACGTGGGCG/ZEN/TCGA/3'IABkFQ/ Integrated DNA Technologies, Inc.

1427

#### 1428 **4K SNP chip genotyping**

1429 Genotyping, including DNA extraction from freeze-dried leaf material, was conducted by  
1430 TraitGenetics (SGS - TraitGenetics GmbH, Germany). *srh1*<sup>P635</sup> mutant, the corresponding wild  
1431 type 'Etincel' and *srh1* pangenome accessions Morex, RGT Planet, HOR 13942, HOR 9043 and  
1432 HOR 21599 were genotyped for background confirmation. Pairwise genetic distance of  
1433 individuals was calculated as the average of their per-locus distances<sup>88</sup> using R package  
1434 stringdist<sup>89</sup> (v 0.9.8). Principal Coordinate Analysis (PCoA) was done with R<sup>64</sup> (v 4.0.2) base  
1435 function cmdscale based on this genetic distance matrix. The first two PCs were illustrated by  
1436 ggplot2 (<https://ggplot2.tidyverse.org>).

1437

#### 1438 **Sanger sequencing**

1439 gDNA of the *srh1*<sup>P635</sup> variant and 'Etincel' was extracted from one-week old seedling leaves  
1440 (DNeasy, Plant Mini Kit, Qiagen, Hilden, Germany). Genomic DNA fragments for sequencing  
1441 were amplified by PCR using gene specific primers (forward primer  
1442 5'TTGCACGATTCAAATGTGGT 3', reverse primer 5' TCACCGGGATCTCTCTGAAT 3') and Taq DNA



1443 Polymerase (NEB) for 35 cycles (initial denaturation at 94°C/3 min followed by 35 cycles of  
1444 94°C/45 s, 55°C/60 s, and 72°C/60 s for extension, with a final extension step of 72°C/10 min).  
1445 PCR products were purified using the NucleoSpin Gel and PCR Clean-Up Kit (Macherey-Nagel  
1446 GmbH & Co. AG, Düren, Germany) according to the manufacturer's instructions. Sanger  
1447 sequencing was done at Eurofins Genomics Germany GmbH using a gene-specific sequencing  
1448 primer (5' AGAACGGAGAGGAGAGAAAGAAG 3').  
1449

#### 1450 **RNA preparation, sequencing, and data analysis**

1451 Rachilla tissues from two contrast groups Morex (short), Barke (long) and Bowman (long) and  
1452 BW-NIL-*srh1* (short) were used for RNA sequencing. The rachilla tissues were collected from  
1453 the central spikelets of the respective genotypes at rachilla hair initiation (RI; Waddington 8.0),  
1454 and elongation (RE; Waddington 9.5) stages. Total RNA was extracted using TRIzol reagent  
1455 (Invitrogen) followed by 2-propanol precipitation. Genomic DNA residues were removed with  
1456 DNase I (NEB, M0303L). High-throughput paired-end sequencing was conducted at Novogene  
1457 Co., Ltd (Cambridge, UK) with Illumina NovaSeq 6000 PE150 Platform. RNAseq reads were  
1458 trimmed for adaptor sequences with Trimmomatic<sup>90</sup> (version 0.39) and the MorexV3 genome  
1459 annotation was used as reference to estimate read abundance with Kallisto<sup>91</sup>. The raw read  
1460 counts were normalized to Transcripts per kilo base per million (TPM) expression levels.  
1461

#### 1462 **mRNA *in situ* hybridization**

1463 *in situ* hybridization was conducted in longitudinal and cross sections derived from whole  
1464 spikelet tissues of Bowman and Morex at rachilla hair elongation developmental stage (W9.5)  
1465 with HvSRH1 sense & antisense probes (124 bp). The *in situ* hybridization was performed as  
1466 described before<sup>92</sup> with few modifications.  
1467

#### 1468 **Code availability**

1469 Scripts for pangenome graphs analyses are available at [https://github.com/mb47/minigraph-](https://github.com/mb47/minigraph-barley)  
1470 [barley](https://github.com/mb47/minigraph-barley). The scripts for calculation of core/shell and cloud genes are deposited to the  
1471 repository <https://github.com/PGSB-HMGU/>. The pipeline for identifying structurally  
1472 complex loci is available at <https://github.com/mtrw/DGS>.  
1473

#### 1474 **Data availability**

1475 All the sequence data collected in this study have been deposited at the European Nucleotide  
1476 Archive (ENA) under BioProjects PRJEB40587, PRJEB57567 and PRJEB58554 (raw data for  
1477 pangenome assemblies), PRJEB64639 (pan-transcriptome Illumina data), PRJEB64637  
1478 (transcriptome Isoseq data), PRJEB53924 (Illumina resequencing data), PRJEB45466-511 (raw  
1479 data for gene space assemblies), PRJEB65284 (*srh1* transcriptome data). Accession codes for  
1480 individual genotypes are listed in supplementary tables: **Supplementary Table 1** (pangenome  
1481 assemblies and associated raw data), **Supplementary Table 2** (transcriptome data),  
1482 **Supplementary Table 5** (Illumina resequencing), **Supplementary Table 6** (gene space  
1483 assemblies).  
1484

#### 1485 **References for Methods**

1486  
1487 1 Dvorak, J., McGuire, P. E. & Cassidy, B. Apparent sources of the A genomes of wheats  
1488 inferred from polymorphism in abundance and restriction fragment length of

- 1489 repeated nucleotide sequences. *Genome* **30**, 680-689 (1988).  
1490 <https://doi.org/10.1139/g88-115>
- 1491 2 Padmarasu, S., Himmelbach, A., Mascher, M. & Stein, N. In Situ Hi-C for Plants: An  
1492 Improved Method to Detect Long-Range Chromatin Interactions. *Methods Mol Biol*  
1493 **1933**, 441-472 (2019). [https://doi.org/10.1007/978-1-4939-9045-0\\_28](https://doi.org/10.1007/978-1-4939-9045-0_28)
- 1494 3 Himmelbach, A., Walde, I., Mascher, M. & Stein, N. Tethered Chromosome  
1495 Conformation Capture Sequencing in Triticeae: A Valuable Tool for Genome  
1496 Assembly. *Bio-protocol* **8**, e2955 (2018). <https://doi.org/10.21769/BioProtoc.2955>
- 1497 4 Himmelbach, A. *et al.* Discovery of multi-megabase polymorphic inversions by  
1498 chromosome conformation capture sequencing in large-genome plant species. *The*  
1499 *Plant Journal* (2018).
- 1500 5 Cheng, H., Concepcion, G. T., Feng, X., Zhang, H. & Li, H. Haplotype-resolved de novo  
1501 assembly using phased assembly graphs with hifiasm. *Nature Methods* **18**, 170-175  
1502 (2021). <https://doi.org/10.1038/s41592-020-01056-5>
- 1503 6 Marone, M. P., Singh, H. C., Pozniak, C. J. & Mascher, M. A technical guide to TRITEX,  
1504 a computational pipeline for chromosome-scale sequence assembly of plant  
1505 genomes. *Plant Methods* **18**, 128 (2022). [https://doi.org/10.1186/s13007-022-00964-](https://doi.org/10.1186/s13007-022-00964-1)  
1506 [1](https://doi.org/10.1186/s13007-022-00964-1)
- 1507 7 Rhie, A., Walenz, B. P., Koren, S. & Phillippy, A. M. Merqury: reference-free quality,  
1508 completeness, and phasing assessment for genome assemblies. *Genome Biology* **21**,  
1509 245 (2020). <https://doi.org/10.1186/s13059-020-02134-9>
- 1510 8 Sun, H., Ding, J., Piednoël, M. & Schneeberger, K. findGSE: estimating genome size  
1511 variation within human and Arabidopsis using k-mer frequencies. *Bioinformatics* **34**,  
1512 550-557 (2017). <https://doi.org/10.1093/bioinformatics/btx637>
- 1513 9 Simão, F. A., Waterhouse, R. M., Ioannidis, P., Kriventseva, E. V. & Zdobnov, E. M.  
1514 BUSCO: assessing genome assembly and annotation completeness with single-copy  
1515 orthologs. *Bioinformatics* **31**, 3210-3212 (2015).  
1516 <https://doi.org/10.1093/bioinformatics/btv351>
- 1517 10 Quinlan, A. R. & Hall, I. M. BEDTools: a flexible suite of utilities for comparing  
1518 genomic features. *Bioinformatics* **26**, 841-842 (2010).  
1519 <https://doi.org/10.1093/bioinformatics/btq033>
- 1520 11 Steinegger, M. & Söding, J. MMseqs2 enables sensitive protein sequence searching  
1521 for the analysis of massive data sets. *Nature Biotechnology* **35**, 1026-1028 (2017).  
1522 <https://doi.org/10.1038/nbt.3988>
- 1523 12 Li, H. Minimap2: pairwise alignment for nucleotide sequences. *Bioinformatics* **1**, 7  
1524 (2018).
- 1525 13 Nattestad, M. & Schatz, M. C. Assemblytics: a web analytics tool for the detection of  
1526 variants from an assembly. *Bioinformatics* **32**, 3021-3023 (2016).  
1527 <https://doi.org/10.1093/bioinformatics/btw369>
- 1528 14 Goel, M., Sun, H., Jiao, W.-B. & Schneeberger, K. SyRI: finding genomic  
1529 rearrangements and local sequence differences from whole-genome assemblies.  
1530 *Genome Biology* **20**, 277 (2019). <https://doi.org/10.1186/s13059-019-1911-0>
- 1531 15 Martin, M. Cutadapt removes adapter sequences from high-throughput sequencing  
1532 reads. *2011* **17**, 3 (2011). <https://doi.org/10.14806/ej.17.1.200>
- 1533 16 Li, H. A statistical framework for SNP calling, mutation discovery, association mapping  
1534 and population genetical parameter estimation from sequencing data. *Bioinformatics*  
1535 **27**, 2987-2993 (2011). <https://doi.org/10.1093/bioinformatics/btr509>

- 1536 17 Zhou, X. & Stephens, M. Genome-wide efficient mixed-model analysis for association  
1537 studies. *Nature Genetics* **44**, 821-824 (2012). [https://doi.org:10.1038/ng.2310](https://doi.org/10.1038/ng.2310)
- 1538 18 Xu, H. *et al.* FastUniq: A Fast De Novo Duplicates Removal Tool for Paired Short Reads.  
1539 *PLOS ONE* **7**, e52249 (2012). [https://doi.org:10.1371/journal.pone.0052249](https://doi.org/10.1371/journal.pone.0052249)
- 1540 19 Bushnell, B., Rood, J. & Singer, E. BBMerge – Accurate paired shotgun read merging  
1541 via overlap. *PLOS ONE* **12**, e0185056 (2017).  
1542 [https://doi.org:10.1371/journal.pone.0185056](https://doi.org/10.1371/journal.pone.0185056)
- 1543 20 Li, H. BFC: correcting Illumina sequencing errors. *Bioinformatics* **31**, 2885-2887  
1544 (2015). [https://doi.org:10.1093/bioinformatics/btv290](https://doi.org/10.1093/bioinformatics/btv290)
- 1545 21 Chikhi, R. & Rizk, G. Space-efficient and exact de Bruijn graph representation based  
1546 on a Bloom filter. *Algorithms for Molecular Biology* **8**, 22 (2013).  
1547 [https://doi.org:10.1186/1748-7188-8-22](https://doi.org/10.1186/1748-7188-8-22)
- 1548 22 Mascher, M. *et al.* Long-read sequence assembly: a technical evaluation in barley.  
1549 *Plant Cell* **33**, 1888-1906 (2021). [https://doi.org:10.1093/plcell/koab077](https://doi.org/10.1093/plcell/koab077)
- 1550 23 Danecek, P. *et al.* Twelve years of SAMtools and BCFtools. *GigaScience* **10** (2021).  
1551 [https://doi.org:10.1093/gigascience/giab008](https://doi.org/10.1093/gigascience/giab008)
- 1552 24 Milner, S. G. *et al.* Genebank genomics highlights the diversity of a global barley  
1553 collection. *Nat Genet* **51**, 319-326 (2019). [https://doi.org:10.1038/s41588-018-0266-](https://doi.org/10.1038/s41588-018-0266-x)  
1554 [x](https://doi.org/10.1038/s41588-018-0266-x)
- 1555 25 Patterson, N., Price, A. L. & Reich, D. Population Structure and Eigenanalysis. *PLOS*  
1556 *Genetics* **2**, e190 (2006). [https://doi.org:10.1371/journal.pgen.0020190](https://doi.org/10.1371/journal.pgen.0020190)
- 1557 26 Jayakodi, M. *et al.* The barley pan-genome reveals the hidden legacy of mutation  
1558 breeding. *Nature* **588**, 284-289 (2020). [https://doi.org:10.1038/s41586-020-2947-8](https://doi.org/10.1038/s41586-020-2947-8)
- 1559 27 Sallam, A. H. *et al.* Genome-Wide Association Mapping of Stem Rust Resistance in  
1560 *Hordeum vulgare* subsp. *spontaneum*. *G3 (Bethesda, Md.)* **7**, 3491-3507 (2017).  
1561 [https://doi.org:10.1534/g3.117.300222](https://doi.org/10.1534/g3.117.300222)
- 1562 28 Chang, C. C. *et al.* Second-generation PLINK: rising to the challenge of larger and  
1563 richer datasets. *GigaScience* **4** (2015). [https://doi.org:10.1186/s13742-015-0047-8](https://doi.org/10.1186/s13742-015-0047-8)
- 1564 29 Rice, P., Longden, I. & Bleasby, A. EMBOSS: the European molecular biology open  
1565 software suite. *Trends in genetics* **16**, 276-277 (2000).
- 1566 30 Letunic, I. & Bork, P. Interactive Tree Of Life (iTOL) v5: an online tool for phylogenetic  
1567 tree display and annotation. *Nucleic Acids Research* **49**, W293-W296 (2021).  
1568 [https://doi.org:10.1093/nar/gkab301](https://doi.org/10.1093/nar/gkab301)
- 1569 31 Dobin, A. *et al.* STAR: ultrafast universal RNA-seq aligner. *Bioinformatics* **29**, 15-21  
1570 (2013). [https://doi.org:10.1093/bioinformatics/bts635](https://doi.org/10.1093/bioinformatics/bts635)
- 1571 32 Kovaka, S. *et al.* Transcriptome assembly from long-read RNA-seq alignments with  
1572 StringTie2. *Genome Biology* **20**, 278 (2019). [https://doi.org:10.1186/s13059-019-](https://doi.org/10.1186/s13059-019-1910-1)  
1573 [1910-1](https://doi.org/10.1186/s13059-019-1910-1)
- 1574 33 Consortium, T. U. UniProt: the Universal Protein Knowledgebase in 2023. *Nucleic*  
1575 *Acids Research* **51**, D523-D531 (2022). [https://doi.org:10.1093/nar/gkac1052](https://doi.org/10.1093/nar/gkac1052)
- 1576 34 Gremme, G., Brendel, V., Sparks, M. E. & Kurtz, S. Engineering a software tool for  
1577 gene structure prediction in higher organisms. *Information and Software Technology*  
1578 **47**, 965-978 (2005). [https://doi.org:https://doi.org/10.1016/j.infsof.2005.09.005](https://doi.org/10.1016/j.infsof.2005.09.005)
- 1579 35 Wu, T. D. & Watanabe, C. K. GMAP: a genomic mapping and alignment program for  
1580 mRNA and EST sequences. *Bioinformatics* **21**, 1859-1875 (2005).  
1581 [https://doi.org:10.1093/bioinformatics/bti310](https://doi.org/10.1093/bioinformatics/bti310)

- 1582 36 Ghosh, S. & Chan, C. K. Analysis of RNA-Seq Data Using TopHat and Cufflinks.  
1583 *Methods Mol Biol* **1374**, 339-361 (2016). [https://doi.org/10.1007/978-1-4939-3167-](https://doi.org/10.1007/978-1-4939-3167-5_18)  
1584 [5\\_18](https://doi.org/10.1007/978-1-4939-3167-5_18)
- 1585 37 Stanke, M. *et al.* AUGUSTUS: ab initio prediction of alternative transcripts. *Nucleic*  
1586 *Acids Research* **34**, W435-W439 (2006). <https://doi.org/10.1093/nar/gkl200>
- 1587 38 Ter-Hovhannisyanyan, V., Lomsadze, A., Chernoff, Y. O. & Borodovsky, M. Gene prediction  
1588 in novel fungal genomes using an ab initio algorithm with unsupervised training.  
1589 *Genome Res* **18**, 1979-1990 (2008). <https://doi.org/10.1101/gr.081612.108>
- 1590 39 Hoff, K. J. & Stanke, M. Predicting Genes in Single Genomes with AUGUSTUS. *Current*  
1591 *Protocols in Bioinformatics* **65**, e57 (2019). <https://doi.org/10.1002/cpbi.57>
- 1592 40 Haas, B. J. *et al.* Automated eukaryotic gene structure annotation using  
1593 EVIDENCEModeler and the Program to Assemble Spliced Alignments. *Genome Biol* **9**,  
1594 R7 (2008). <https://doi.org/10.1186/gb-2008-9-1-r7>
- 1595 41 Haas, B. J. *et al.* Improving the Arabidopsis genome annotation using maximal  
1596 transcript alignment assemblies. *Nucleic Acids Research* **31**, 5654-5666 (2003).  
1597 <https://doi.org/10.1093/nar/gkg770>
- 1598 42 Altschul, S. F., Gish, W., Miller, W., Myers, E. W. & Lipman, D. J. Basic local alignment  
1599 search tool. *J Mol Biol* **215**, 403-410 (1990). [https://doi.org/10.1016/S0022-](https://doi.org/10.1016/S0022-2836(05)80360-2)  
1600 [2836\(05\)80360-2](https://doi.org/10.1016/S0022-2836(05)80360-2)
- 1601 43 Spannagl, M. *et al.* PGSB PlantsDB: updates to the database framework for  
1602 comparative plant genome research. *Nucleic Acids Res* **44**, D1141-1147 (2016).  
1603 <https://doi.org/10.1093/nar/gkv1130>
- 1604 44 Fu, L., Niu, B., Zhu, Z., Wu, S. & Li, W. CD-HIT: accelerated for clustering the next-  
1605 generation sequencing data. *Bioinformatics* **28**, 3150-3152 (2012).  
1606 <https://doi.org/10.1093/bioinformatics/bts565>
- 1607 45 Cock, P. J. *et al.* Biopython: freely available Python tools for computational molecular  
1608 biology and bioinformatics. *Bioinformatics* **25**, 1422-1423 (2009).  
1609 <https://doi.org/10.1093/bioinformatics/btp163>
- 1610 46 Henikoff, S. & Henikoff, J. G. Amino acid substitution matrices from protein blocks.  
1611 *Proceedings of the National Academy of Sciences* **89**, 10915-10919 (1992).  
1612 <https://doi.org/10.1073/pnas.89.22.10915>
- 1613 47 Emms, D. M. & Kelly, S. OrthoFinder: phylogenetic orthology inference for  
1614 comparative genomics. *Genome Biology* **20**, 238 (2019).  
1615 <https://doi.org/10.1186/s13059-019-1832-y>
- 1616 48 Lovell, J. T. *et al.* GENESPACE tracks regions of interest and gene copy number  
1617 variation across multiple genomes. *eLife* **11**, e78526 (2022).  
1618 <https://doi.org/10.7554/eLife.78526>
- 1619 49 Li, H., Feng, X. & Chu, C. The design and construction of reference pangenome graphs  
1620 with minigraph. *Genome Biology* **21**, 265 (2020). [https://doi.org/10.1186/s13059-](https://doi.org/10.1186/s13059-020-02168-z)  
1621 [020-02168-z](https://doi.org/10.1186/s13059-020-02168-z)
- 1622 50 Garrison, E. *et al.* Building pangenome graphs. *bioRxiv*, 2023.2004.2005.535718  
1623 (2023). <https://doi.org/10.1101/2023.04.05.535718>
- 1624 51 Hickey, G. *et al.* Pangenome graph construction from genome alignments with  
1625 Minigraph-Cactus. *Nature Biotechnology* (2023). [https://doi.org/10.1038/s41587-](https://doi.org/10.1038/s41587-023-01793-w)  
1626 [023-01793-w](https://doi.org/10.1038/s41587-023-01793-w)
- 1627 52 Mascher, M. *et al.* Long-read sequence assembly: a technical evaluation in barley.  
1628 *Plant Cell* (2021). <https://doi.org/10.1093/plcell/koab077>



- 1629 53 Garrison, E. *et al.* Variation graph toolkit improves read mapping by representing  
1630 genetic variation in the reference. *Nature Biotechnology* **36**, 875-879 (2018).  
1631 <https://doi.org/10.1038/nbt.4227>
- 1632 54 Guarracino, A., Heumos, S., Nahnsen, S., Prins, P. & Garrison, E. ODGI: understanding  
1633 pangenome graphs. *Bioinformatics* **38**, 3319-3326 (2022).  
1634 <https://doi.org/10.1093/bioinformatics/btac308>
- 1635 55 Park, S.-C., Lee, K., Kim, Y. O., Won, S. & Chun, J. Large-Scale Genomics Reveals the  
1636 Genetic Characteristics of Seven Species and Importance of Phylogenetic Distance for  
1637 Estimating Pan-Genome Size. *Frontiers in Microbiology* **10** (2019).  
1638 <https://doi.org/10.3389/fmicb.2019.00834>
- 1639 56 Sirén, J. *et al.* Pangenomics enables genotyping of known structural variants in 5202  
1640 diverse genomes. *Science* **374**, abg8871 (2021).  
1641 <https://doi.org/doi:10.1126/science.abg8871>
- 1642 57 Li, H. Aligning sequence reads, clone sequences and assembly contigs with BWA-  
1643 MEM. *arXiv preprint arXiv:1303.3997* (2013).
- 1644 58 Rabanus-Wallace, M. T., Wicker, T. & Stein, N. Replicators, genes, and the C-value  
1645 enigma: High-quality genome assembly of barley provides direct evidence that self-  
1646 replicating DNA forms 'cooperative' associations with genes in arms races. *bioRxiv*,  
1647 2023.2010.2001.560391 (2023). <https://doi.org/10.1101/2023.10.01.560391>
- 1648 59 Harris, R. S. *Improved pairwise alignment of genomic DNA*. (The Pennsylvania State  
1649 University, 2007).
- 1650 60 Edgar, R. C. Search and clustering orders of magnitude faster than BLAST.  
1651 *Bioinformatics* **26**, 2460-2461 (2010). <https://doi.org/10.1093/bioinformatics/btq461>
- 1652 61 Ma, J. & Bennetzen, J. L. Rapid recent growth and divergence of rice nuclear  
1653 genomes. *Proceedings of the National Academy of Sciences* **101**, 12404-12410  
1654 (2004). <https://doi.org/doi:10.1073/pnas.0403715101>
- 1655 62 Buchmann, J. P., Matsumoto, T., Stein, N., Keller, B. & Wicker, T. Inter-species  
1656 sequence comparison of Brachypodium reveals how transposon activity corrodes  
1657 genome colinearity. *The Plant Journal* **71**, 550-563 (2012).  
1658 [https://doi.org:https://doi.org/10.1111/j.1365-313X.2012.05007.x](https://doi.org/https://doi.org/10.1111/j.1365-313X.2012.05007.x)
- 1659 63 Kuraku, S., Zmasek, C. M., Nishimura, O. & Katoh, K. aLeaves facilitates on-demand  
1660 exploration of metazoan gene family trees on MAFFT sequence alignment server  
1661 with enhanced interactivity. *Nucleic Acids Research* **41**, W22-W28 (2013).  
1662 <https://doi.org/10.1093/nar/gkt389>
- 1663 64 R Core Team. R: A language and environment for statistical computing. R Foundation  
1664 for Statistical Computing, Vienna, Austria. 2022. (2022).
- 1665 65 Untergasser, A. *et al.* Primer3—new capabilities and interfaces. *Nucleic Acids*  
1666 *Research* **40**, e115-e115 (2012). <https://doi.org/10.1093/nar/gks596>
- 1667 66 Danecek, P. *et al.* The variant call format and VCFtools. *Bioinformatics* **27**, 2156-2158  
1668 (2011). <https://doi.org/10.1093/bioinformatics/btr330>
- 1669 67 Marçais, G. & Kingsford, C. A fast, lock-free approach for efficient parallel counting of  
1670 occurrences of k-mers. *Bioinformatics* **27**, 764-770 (2011).  
1671 <https://doi.org/10.1093/bioinformatics/btr011>
- 1672 68 Kadziola, A., Sjøgaard, M., Svensson, B. & Haser, R. Molecular structure of a barley  
1673 alpha-amylase-inhibitor complex: implications for starch binding and catalysis. *J Mol*  
1674 *Biol* **278**, 205-217 (1998). <https://doi.org/10.1006/jmbi.1998.1683>



- 1675 69 Rodrigues, C. H. M., Pires, D. E. V. & Ascher, D. B. DynaMut2: Assessing changes in  
1676 stability and flexibility upon single and multiple point missense mutations. *Protein*  
1677 *Science* **30**, 60-69 (2021). [https://doi.org:https://doi.org/10.1002/pro.3942](https://doi.org/10.1002/pro.3942)
- 1678 70 WADDINGTON, S. R., CARTWRIGHT, P. M. & WALL, P. C. A Quantitative Scale of Spike  
1679 Initial and Pistil Development in Barley and Wheat. *Annals of Botany* **51**, 119-130  
1680 (1983). [https://doi.org:10.1093/oxfordjournals.aob.a086434](https://doi.org/10.1093/oxfordjournals.aob.a086434)
- 1681 71 Poursarebani, N. *et al.* The Genetic Basis of Composite Spike Form in Barley and  
1682 'Miracle-Wheat'. *Genetics* **201**, 155-165 (2015).  
1683 [https://doi.org:10.1534/genetics.115.176628](https://doi.org/10.1534/genetics.115.176628)
- 1684 72 Beier, S. *et al.* Construction of a map-based reference genome sequence for barley,  
1685 *Hordeum vulgare* L. *Scientific Data* **4**, 170044 (2017).  
1686 [https://doi.org:10.1038/sdata.2017.44](https://doi.org/10.1038/sdata.2017.44)
- 1687 73 Taylor, J. & Butler, D. R Package ASMap: Efficient Genetic Linkage Map Construction  
1688 and Diagnosis. *Journal of Statistical Software* **79**, 1 - 29 (2017).  
1689 [https://doi.org:10.18637/jss.v079.i06](https://doi.org/10.18637/jss.v079.i06)
- 1690 74 Wu, Y., Bhat, P. R., Close, T. J. & Lonardi, S. Efficient and Accurate Construction of  
1691 Genetic Linkage Maps from the Minimum Spanning Tree of a Graph. *PLOS Genetics* **4**,  
1692 e1000212 (2008). [https://doi.org:10.1371/journal.pgen.1000212](https://doi.org/10.1371/journal.pgen.1000212)
- 1693 75 Broman, K. W., Wu, H., Sen, Ś. & Churchill, G. A. R/qtl: QTL mapping in experimental  
1694 crosses. *Bioinformatics* **19**, 889-890 (2003).  
1695 [https://doi.org:10.1093/bioinformatics/btg112](https://doi.org/10.1093/bioinformatics/btg112)
- 1696 76 Dempster, A. P., Laird, N. M. & Rubin, D. B. Maximum likelihood from incomplete data  
1697 via the EM algorithm. *Journal of the royal statistical society: series B (methodological)*  
1698 **39**, 1-22 (1977).
- 1699 77 Pidon, H. *et al.* High-resolution mapping of Rym14Hb, a wild relative resistance gene  
1700 to barley yellow mosaic disease. *Theoretical and Applied Genetics* **134**, 823-833  
1701 (2021). [https://doi.org:10.1007/s00122-020-03733-7](https://doi.org/10.1007/s00122-020-03733-7)
- 1702 78 Camacho, C. *et al.* BLAST+: architecture and applications. *BMC Bioinformatics* **10**, 421  
1703 (2009). [https://doi.org:10.1186/1471-2105-10-421](https://doi.org/10.1186/1471-2105-10-421)
- 1704 79 Edgar, R. C. Muscle5: High-accuracy alignment ensembles enable unbiased  
1705 assessments of sequence homology and phylogeny. *Nature Communications* **13**,  
1706 6968 (2022). [https://doi.org:10.1038/s41467-022-34630-w](https://doi.org/10.1038/s41467-022-34630-w)
- 1707 80 Rice, P., Longden, I. & Bleasby, A. EMBOSS: the European Molecular Biology Open  
1708 Software Suite. *Trends Genet* **16**, 276-277 (2000). [https://doi.org:10.1016/s0168-](https://doi.org/10.1016/s0168-9525(00)02024-2)  
1709 [9525\(00\)02024-2](https://doi.org/10.1016/s0168-9525(00)02024-2)
- 1710 81 Chen, Y. & Wang, X. Evaluation of efficiency prediction algorithms and development  
1711 of ensemble model for CRISPR/Cas9 gRNA selection. *Bioinformatics* **38**, 5175-5181  
1712 (2022). [https://doi.org:10.1093/bioinformatics/btac681](https://doi.org/10.1093/bioinformatics/btac681)
- 1713 82 Gruber, A. R., Lorenz, R., Bernhart, S. H., Neuböck, R. & Hofacker, I. L. The Vienna  
1714 RNA websuite. *Nucleic Acids Res* **36**, W70-74 (2008).  
1715 [https://doi.org:10.1093/nar/gkn188](https://doi.org/10.1093/nar/gkn188)
- 1716 83 Koepfel, I., Hertig, C., Hoffie, R. & Kumlehn, J. Cas Endonuclease Technology—A  
1717 Quantum Leap in the Advancement of Barley and Wheat Genetic Engineering.  
1718 *International Journal of Molecular Sciences* **20**, 2647 (2019).
- 1719 84 Gerasimova, S. V. *et al.* Conversion of hulled into naked barley by Cas endonuclease-  
1720 mediated knockout of the NUD gene. *BMC Plant Biology* **20**, 255 (2020).  
1721 [https://doi.org:10.1186/s12870-020-02454-9](https://doi.org/10.1186/s12870-020-02454-9)

- 1722 85 Hensel, G., Kastner, C., Oleszczuk, S., Riechen, J. & Kumlehn, J. Agrobacterium-  
1723 mediated gene transfer to cereal crop plants: current protocols for barley, wheat,  
1724 triticale, and maize. *Int J Plant Genomics* **2009**, 835608 (2009).  
1725 <https://doi.org/10.1155/2009/835608>
- 1726 86 Watson, A. *et al.* Speed breeding is a powerful tool to accelerate crop research and  
1727 breeding. *Nature Plants* **4**, 23-29 (2018). <https://doi.org/10.1038/s41477-017-0083-8>
- 1728 87 Knudsen, S. *et al.* FIND-IT: Accelerated trait development for a green evolution.  
1729 *Science Advances* **8**, eabq2266 (2022). <https://doi.org/doi:10.1126/sciadv.abq2266>
- 1730 88 Witherspoon, D. J. *et al.* Genetic similarities within and between human populations.  
1731 *Genetics* **176**, 351-359 (2007). <https://doi.org/10.1534/genetics.106.067355>
- 1732 89 Van der Loo, M. P. The stringdist package for approximate string matching. *R J.* **6**, 111  
1733 (2014).
- 1734 90 Bolger, A. M., Lohse, M. & Usadel, B. Trimmomatic: a flexible trimmer for Illumina  
1735 sequence data. *Bioinformatics* **30**, 2114-2120 (2014).  
1736 <https://doi.org/10.1093/bioinformatics/btu170>
- 1737 91 Bray, N. L., Pimentel, H., Melsted, P. & Pachter, L. Near-optimal probabilistic RNA-seq  
1738 quantification. *Nature biotechnology* **34**, 525-527 (2016).
- 1739 92 Poursarebani, N. *et al.* COMPOSITUM 1 contributes to the architectural simplification  
1740 of barley inflorescence via meristem identity signals. *Nature Communications* **11**,  
1741 5138 (2020). <https://doi.org/10.1038/s41467-020-18890-y>
- 1742 93 Arend, D. *et al.* PGP repository: a plant phenomics and genomics data publication  
1743 infrastructure. *Database* **2016** (2016).  
1744  
1745  
1746